Robust Techniques and Stochastic Resonance for Segmentation of Noisy Images

A thesis submitted to the University of Hyderabad in partial fulfillment of the requirements for the award of

Doctor of Philosophy

in

Computer Science

by

J.V.R.Sagar

School of Computer and Information Sciences

University of Hyderabad

Hyderabad – 500 046, India

September 2013

CERTIFICATE

This is to certify that the thesis entitled **Robust Techniques and Stochastic Resonance for Segmentation of Noisy Images** submitted by **J.V.R.Sagar** bearing Reg. No **01MCPC03** in partial fulfillment of the requirements for the award of **Doctor of Philosophy** in **Computer Science** is a bonafide work carried out by him under my supervision and guidance.

The thesis has not been submitted previously in part or in full to this or any other University or Institution for the award of any degree or diploma.

Prof. Chakravarthy Bhagvati

(Supervisor)

School of CIS

University of Hyderabad

Hyderabad - 500046

Dean

School of CIS

University of Hyderabad

Hyderabad - 500046

DECLARATION

I, J.V.R.Sagar hereby declare that this thesis entitled **Robust Techniques and Stochastic Resonance for Segmentation of Noisy Images** submitted by me under the guidance and supervision of **Prof. Chakravarthy Bhagvati** is a bonafide research work. I also declare that it has not been submitted previously in part or in full to this University or any other University or Institution for the award of any degree or diploma.

Date:

Name : J.V.R.Sagar

Regd. No. 01MCPC03

Signature of the student

Acknowledgment

I would like to express my deep sense of gratitude to my research supervisor Prof. Chakravarthy Bhagvati for his inspiration, continuous guidance, support and encouragement in carrying out this work. I express my sincere thanks to Prof. A K Pujari, Dean, School of Computer and Information Sciences for his constant motivation and valuable suggestions at different stages of the research work.

I would also like to convey my sincere thanks to Prof. BL Deekshatulu, Distinguished Fellow,IDRBT, Prof. Atul Negi, Dr S Durga Bhavani and Dr P Anupama, faculty at SCIS for their useful ideas and motivating words. I sincerely acknowledge the support given by Shri Sibnath Som, Director, DRDL for pursuing the work. I also thank my colleagues at DRDL, Dr BS Subhash Chandran, Dr AK Sarkar and Shri S Venugopal for the encouragement given to me.

I gratefully thank my father and mother who constantly encouraged and inspired me to work hard in difficult times and achieve my goals. I would also like to acknowledge the support and patience shown by my wife,Asha, and sons Arun and Shyam in these years.

Abstract

The broad problem addressed in the thesis is the segmentation of noisy and low contrast images. Detecting and preserving weak features is also a goal of this work. Such applications occur frequently in medical, remote sensing images, military and surveillance domains. The ultimate motivation of the research work is the development of a new class of algorithms which will autonomously interpret the visual environment and match the human eye in performance. Stated more formally the goal is to segment images with low signal-to-noise ratio (SNR). A multi-pronged approach that includes the following specific tasks is developed for the segmentation problem.

- Systematically studying the performance of robust techniques in general and mean shift filter (MSF) in particular.
- Finding the limits of mean shift filter.
- Identifying or discovering techniques that perform beyond mean shift filter.
- Studying stochastic resonance (SR) as a complementary approach to robust statistics.

The research focuses on the development of robust techniques for detecting weak features in images contaminated with Gaussian noise and images having low contrast features. A research survey of current techniques indicated that robust techniques are useful in handling noisy signals and tolerate noise better than conventional techniques. The survey also led to an exploration of unconventional techniques which are capable of boosting weak signals. The need to bridge the gap between these two altogether different techniques was felt and the contribution of this research was to develop an integrated approach for segmenting images with low signal-to-noise ratio (SNR). The approach to integrate two different techniques has led to development of a new technique which aims to reduce the effect of noise and boost the signal in a noisy image thus leading to a new paradigm in treating the segmentation problem as a combination of two complementary techniques- one for boosting the weak signal and the other for handling the noise.

As a part of the work a database of 160 clean and noisy images is created for testing the segmentation algorithms. The systematic study of mean shift filtering

led to the development of four new variants. The results of their performance revealed that mean shift filter and its variants are capable of handling Gaussian noise less than 20%. However, a combination of mean shift filter and stochastic resonance showed that higher amounts of noise (30% and in some cases even 50%) may also be handled. Moreover, SR allows weak features to be boosted in strength and consequently be preserved. It is concluded that SR and mean shift filter are complementary and the proposed approach combining them may be seen as a preliminary step for developing a new family of algorithms that go beyond robust techniques for segmentation.

The major contributions of the research work can be listed as follows.

- Combining robust techniques with SR and showing that the combination can handle images which are not handled by either of the two separately.
- Developing a segmentation algorithm that combines SR with mean shift filter.
- To suggest SR as a new approach or paradigm that is complimentary to robust techniques in handling low SNR images.
- Development of four variants of the mean shift filter and their performance analysis.
- A systematic study of mean shift filter, its parameters and limitations.

Contents

List of Tables

List of Figures

Symbols

K	Kernel
h	Kernel radius
R^d	Euclidean space of d dimensions
n	number of sample points
$M_h(x)$	Mean shift for sample x
σ_s	Normalisation constant in the spatial domain
σ_r	Normalisation constant in the range domain
$S_h(x)$	Hypersphere of radius h and centered on x
c_d	Volume of the unit d-dimensional sphere
μ	Mean
σ	Standard deviation
$T1$	Lower threshold of variance
$T2$	Upper threshold of variance
$s(t)$	Signal
a	Detectability threshold
$\mu_2(k)$	Kernel constant
$R(k)$	Kernel constant
$p(t)$	Kernel estimator
$\phi()$	Normal cumulative distribution function
$\psi()$	Normal probability density function

Abbreviations

MSF	Mean Shift Filter
AMISE	Asymptotic Mean Integrated Square Error
SNR	Signal-to-Noise Ratio
PSNR	Peak Signal-to-Noise Ratio
SR	Stochastic Resonance
SB	Stochastic Bucket
AMASE	Asymptotic Mean Average Square Error

Chapter 1

Introduction

1.1 Problem Definition

The basic problem for the research work done was the segmentation of noisy and low contrast images. Segmentation is the process of subdividing an image into constituent parts like objects, regions containing pixels of similar properties and contiguous regions. It is one of the most important steps in image processing. Segmentation splits an image I into *regions* or subsets R_i with the following properties.

$I = \bigcup_{i=1}^{N} R_i$: all pixels belong to some segment or the other.

$R_i \cap R_j = \phi, i \neq j$: regions do not overlap.

Each R_i is a *connected component*, i.e., there exists a path that lies entirely within R_i between every pair of pixels.

Finding regions that represent objects or meaningful parts of the objects in the image is the goal of image segmentation. By segmentation it is possible to identify real objects, pseudo objects, shadows or other regions of interest. Image segmentation algorithms generally use one of the two basic properties of intensity value : discontinuity and similarity [1]. In the discontinuity -based approach, the image is partitioned based on abrupt changes in intensity such as edges in an image. In the similarity based approach the image is partitioned into regions that are similar according to some criteria like gray level, color,texture or some statistical property. Conventional segmentation techniques use one of the two approaches. Discontinuity based and similarity based techniques are dual techniques . While one approach focuses on continuity, the other on discontinuity . Each of these

approaches misses half of the available information [2].

While it is easy to state or conceptualize segmentation for images , there are practical problems when images are contaminated with noise and/or have low contrast. In this context, the signal-to-noise ratio (SNR) of an image is an important parameter which measures the image quality. High values being "good". Most practical images of interest are contaminated with noise. Examples are medical images, remotely sensed images, military images etc. These images have an additional feature of being low contrast also. This research work is focussed on the Mean Shift filter which has been successfully used for many segmentation applications in the last decade.

1.2 Motivation

Irrespective of whether it is a computer vision application or an image processing application one common task is image analysis. Image analysis involves the examination of the image data to facilitate solving an image problem [3]. It is concerned with the investigation of the data present in an image for a specific application. The image analysis attempts to gain insight into the images by using the raw data as input and determines how to use the data to extract the information that is needed. The image analysis task makes use of tools like image segmentation, image transforms, feature extraction and pattern classification [3]. Several research groups have studied the fundamental problem of segmentation in the last four decades. The evolution of segmentation in this period has led to several types of techniques. These techniques can be categorized into the following seven broad groups.

- Basic techniques including thresholding and ranging, edge detection and connected components.
- Region based techniques including region growing, splitting and split-and-merge.
- Morphological techniques like conditional dilation, closing and watersheds.
- Clustering techniques like k-means, nearest neighbor and neural networks.
- Graph based techniques like spanning tree and normalized cuts.

- Transform domain techniques like Fourier transform, wavelets and Gabor filters.

- Robust techniques

Considering that images of interest are inherently noisy and low contrast in nature, there was a strong motivation for carrying out research in robust techniques for detecting features in noisy and low contrast images. Features in images which are weak in strength, to be detected using conventional edge detection techniques were of special interest. In [4] robust algorithms are defined as follows : "Robust algorithms should be able to handle noisy data and identify approximate patterns. They should therefore tolerate a small amount of noise in the sense that it will not affect their output too much. We describe an algorithm with this property as robust". As mentioned in [5] the ultimate goal of computer vision is to make possible systems that can autonomously interpret the visual environment under almost any operating condition, to reproduce the amazing performance of human visual perception. The research survey in current techniques indicated that robust techniques are useful in handling noisy signals and essentially tolerate noise in a better way than conventional techniques. The survey also indicated the use of unconventional techniques which are capable of boosting weak signals. The need to bridge the gap between these two altogether different techniques was felt and the contribution of this research was to develop an integrated approach for improving the signal-to-noise ratio (SNR) of noisy images. The ultimate motivation of the research work was the development of a new class of algorithms which will lead to capabilities similar to the human visual perception in the future.

1.3 Objectives

The broad objective of the research work was to segment images with high noise and low contrast. Stated differently, the goal was to segment images with low signal-to-noise ratio (SNR). Elucidating further, the specific objectives are as mentioned below.

- Systematic study of robust techniques in general and mean shift filter in particular for their performance in segmenting low SNR images.

- Finding the limits of mean shift filter.
- Identify or discover techniques that perform beyond robust statistics.
- Study Stochastic Resonance(SR) as a complementary approach to robust statistics.

1.4 Approach

The approach used in the research was to merge both these approaches to get the advantages of both and also use robust techniques to get an overall improvement in the ability to detect and segment weak features in noisy and low contrast images. Gaussian noise is a very good approximation to noise that occurs in many practical cases [6]. Hence, only Gaussian noise contaminated images were considered as candidate images.The approach used for the research work can be identified into the following three major points.

- Benchmark image dataset contaminated with Gaussian noise of varying magnitude has been created and the mean shift filter applied and evaluated.
- Modify the mean shift filter and again study its performance on these contaminated images.
- For the failure cases of the mean shift filter, identify the complementary approaches to segment them.

1.5 Contributions

The research is focussed on the development of robust techniques for detecting weak features in images contaminated with Gaussian noise and images having low contrast features. The approach to integrate two different techniques has led to development of a new technique which aims to reduce the effect of noise and boost the signal in a noisy image thus leading to a new paradigm in treating the segmentation problem as a combination of two complementary techniques- one for handling the weak signal and the other for handling the noise.
The major contributions of the research work can be listed as follows.

1. Combining robust techniques with SR and showing that the combination can handle images which are not handled by either of the two separately.
    - Developing a segmentation algorithm that combines SR with mean shift filter.
    - To suggest SR as a new approach or paradigm that is complementary to robust techniques in handling low SNR images.
    - Development of four variants of the mean shift filter and their performance analysis.
2. A thorough study of mean shift filter and its parameters.
3. Finding the limitations of mean shift filter.

1.6 Thesis Outline

Chapter 2 presents a survey of the current robust techniques including stochastic resonance. Chapter 3 discusses the mean shift filter and its characteristics. The study of the mean shift filter on noisy images is presented in Chapter 4. The integration of stochastic resonance and mean shift filter is discussed in Chapter 5. The discussions and conclusions are given in Chapter 6.

Chapter 2

Algorithms for segmenting noisy images

The inability to make computer vision systems which can match the human perception in interpreting the visual environment when different levels of noise are present led to the development of robust techniques. This chapter introduces robust techniques and describes a few important algorithms for segmentation of low SNR images. The initial sections introduce robustness, its role in computer vision, robust estimators, techniques from statistics, clustering techniques, non parametric estimation techniques including the mean shift filter and stochastic resonance. The conclusions at the end of the chapter present the applicability of these algorithms, limitations, un-addressed areas in these algorithms and scope for research as a prelude to our work presented in the succeeding chapters.

2.1 What is a robust technique ?

A robust technique can be defined on the notion of a "breakdown point" [5]. Any technique can tolerate noise in an image. This noise is due to pixels called outliers. The performance of a technique degrades with increasing noise until a breakdown stage is reached. This breakdown point is defined in terms of the smallest fraction of outliers which cause the technique to produce arbitrarily bad quality results. Robust techniques are those which can handle significantly higher outlier percentage without breaking down. Thus median of a sample dataset is more robust than the mean since the breakdown occurs only if more than 50% of

the sample set are outliers whereas for the mean, even a single large outlier could potentially cause a large error in the estimate. Robust statistical methods were first adopted in computer vision to improve the performance of feature extraction algorithms at the bottom level of the vision hierarchy [5].

2.2 Role of Robustness in Computer Vision

As mentioned in [7], the characteristics of the visual signal such as the overwhelming amount of data, high redundancy, relevant information clustered in space and time, indicate that certain organization and aggregation principles have to be used to reduce the computational complexity of the visual processes and to bridge the gap between the raw data and symbolic descriptions. In computer vision, the data aggregation problem is most commonly approached by fitting models of visual phenomena to image data. Because the image data is inherently unreliable a fitting method should be able to cope with both :

1. noise that is well-behaved in a distributional sense and
2. outliers which are either large measurement errors or data points belonging to other distributions (models).

The least-squares estimator that assumes a pure Gaussian noise is very sensitive to outliers in the data set leading to extremely poor results. In [7] it is argued that visual perception is fundamentally a problem in discrimination. Data must be combined with similar data and outliers must be rejected. In other words, vision algorithms must be able to combine data while simultaneously discriminating between data that should be kept distinct, such as outliers(errors) and data from other regions. In fact the data association problem (grouping) makes the task of machine perception fundamentally different from the traditional estimation problems.

2.3 Robust estimators

The estimators that remain stable in the presence of various types of noise and can tolerate a certain portion of outliers are known under the generic name of

robust estimators [8]. The use of robust estimators in computer vision is to reject outliers than to optimally estimate parameters of the model. This is especially so in the case of non-Gaussian data distributions that may arise from the nature of the physical data.

2.4 Measures of Robustness

Some of the important measures of robustness used for judging the efficacy of a robust technique are described below.

1. Breakdown point

   This is the minimum fraction of outlying data that can cause an estimate to diverge arbitrarily far from the true estimate. If the sample size is n then the breakdown point for the mean is $1/n$ and that for the median is 50% of n. This was first proposed by Hodges in 1967.

2. Influence function

   Proposed by Hampel in 1974 [42], this is the change in an estimate caused by insertion of outlying data as a function of the distance of the outlier from the un-corrupted estimate. To achieve robustness, the influence function should tend to zero with increasing distance.

3. Efficiency

   This is the ratio of the minimum possible variance in an estimate to the actual variance of the robust estimate.

2.5 Robust parameter estimation

Extracting geometric, photometric and semantic information from an image data is an important goal for computer vision algorithms [8]. The processes that are used for extraction of this information need the use of parameter estimation techniques to describe intensity edge curves, motion models, surface normals and curvatures, Euclidean, affine and projective transformation models [8]. In parallel with the use of parameter estimation techniques, segmentation of the image data into distinct populations is an area which has received attention of the computer

vision researchers. As mentioned in [8], complete segmentation is not possible without parameter estimation as the process of assigning data points to populations depends at least partially on the parameters describing the structure of each population. Thus identifying whether a pixel belongs to a particular edge or a region in an image is impossible unless the parameters of the edge or region are known or are correctly estimated. It is precisely this particular difficulty which led to research in robust parameter estimation techniques. Contribution to these techniques are from both the computer vision community and the statistics community. The main reason for choosing robust image segmentation as the topic for this thesis work was [this "chick-and-egg" problem] the challenge of correctly identifying edge pixels and regions in the context of noisy images. Considering the fact that robust techniques have been designed to handle outliers and multiple populations, the literature survey carried out as part of the thesis work is focussed on these techniques.

The performance of robust estimators is assessed by objective functions which are defined in terms of an error distance or residual function which could be the geometric distance a set of data points and the parameter vector(for the data set) which is being estimated. Robust estimation techniques have been contributed by the statistics community and the computer vision researchers.

2.6 Statistical techniques

Two of the most significant robust estimation techniques are the M-estimators and the Least Median of Squares (LMS). M-estimators generalize the maximum likelihood estimator and the least squares estimator. In least square regression, all data points have equal weights. When outliers are present, there will be considerable bias and rapid deterioration of the quality of the estimate. In contrast to this, adaptive weighting is used in M-estimation. The influence from a data point is decreased when the noise at that point is large. Influence functions used are those suggested by Beaton & Tukey, Huber, Andrews, Hampel and Cauchy [42, 41]. Least median of squares (LMS) has a breakdown point of 0.5 which is the highest. Upto half the data points can be far off from the optimum estimate without changing the objective function value. As the median is not differentiable, alternative techniques for finding the least value of the median of squares in the

LMS technique need to be used.

2.7 Computer Vision Techniques

Some of the major algorithms in computer vision are the Hough Transform, RANSAC algorithm, MINPRAN, MUSE and ALKS. The Hough transform [9] is considered the most successful general-purpose vision algorithm [5]. The technique provides robustness against outliers by placing them in cells which have less significance by virtue of having fewer votes from the pixels in the image domain. In the RANSAC method [10], a small subset of points is chosen and a fit is made to that subset. The conformance of the remaining points to this fit is checked. This process is continued until there is a high probability of finding the stucture that is sought for. Thus this technique is a search for a random sample that leads to a fit on which many of the data points agree and is called Random Sample Consensus(RANSAC). MINPRAN [11] is a robust estimator. This estimator does not assume that there is a known limit for the error of the good data in the image. It uses random sampling to search for the fit and the number of inliers to the fit that are least likely to have occurred randomly. Thus it is capable of obtaining good fits even when the percentage of outliers is greater than 50%. MUSE [12] is an acronym for Minimum Unbiased Scale Estimator. This estimator is based on the premise that the robust estimators which are successful in extracting a single signal corrupted with random outliers are not suitable for extracting multiple surfaces in an image region and fail to tolerate discontinuities between the multiple surfaces. The ALKS (Adaptive Least K^{th} order Squares) estimator [13] minimizes the K^{th} order statistics of the squared residuals. The least K^{th} order chooses a p-tuple randomly from the data to define a model hypothesis ($p < k < n$). The residuals of this partial model u_i are computed. The residuals are then sorted in ascending order and the location of the shortest window containing at least k residuals is found. The procedure is repeated for several p-tuples and the p-tuple yielding the smallest window provides the LKS estimate of the model.

2.8 Other Robust Techniques

Having surveyed the robust techniques from statistics and computer vision for noise and outlier handling capabilities, further survey was carried out to identify other robust techniques which could be considered for use on noisy images. Among the other robust techniques, clustering techniques have been used extensively in pattern recognition, computer vision and control tasks. These techniques have been used for detection of clusters of various shapes such as lines, planes, circles, ellipses, curves and curved surfaces. In [15, 16, 17, 18, 19, 20, 21]these techniques are presented. However, to handle practical applications these clustering techniques need to be robust and a number of new techniques [22, 23, 24, 25, 26, 27, 28] have been developed. These techniques claim robustness to noise and outliers to varying levels. Among these techniques the fuzzy clustering approach has been an area of active research.This is because of two reasons. The concept of weight functions in robust statistics can be related to the concept of membership functions in fuzzy set theory. A fuzzy approach is more tolerant to variations and noise in the input data compared to a crisp approach as claimed by researchers.

2.9 Clustering Techniques

Clustering is a type of classification imposed on a finite set of objects and the relationship between the objects is represented in a proximity matrix in which rows and columns correspond to objects [29]. Traditional clustering algorithms can be divided into two main categories : hierarchical and partitional. In hierarchical clustering, the number of clusters need not be specified a priori and problems due to initialization and local minima do not arise. However since these methods consider only local neighbors in each step they cannot incorporate a priori knowledge about the global shape or size of clusters. Therefore, these techniques cannot always separate overlapping clusters. Further, the points are static in the sense that once allotted to a particular cluster, they cannot move to a different cluster. In contrast, partitional clustering algorithms are dynamic and the data points can move from one cluster to another. They can incorporate knowledge about the shape or size of clusters by using appropriate prototypes and distance

measures. Two major drawbacks of the partitional approach are the difficulty in determining the number of clusters and the sensitivity to noise and outliers. Some of the important robust clustering techniques that were surveyed are described here. The survey indicated that the important algorithms based on this method are as mentioned below

1. The Ohashi algorithm [27]. This algorithm attempts to handle the problem of noise sensitivity in Fuzzy C means algorithm by introducing an objective function where the membership of a point in the class of outliers and a resolution parameter α is used. The algorithm minimizes the function in the process of clustering. The problem with this algorithm is the need to correctly specify the value of α.

2. Noise clustering(NC) method [22, 23]. This algorithm proposes the idea of a noise cluster to deal with noisy data. The noise is considered to be a separate class and is represented by a prototype that has a constant distance δ from all the data points. The membership u_{*j} of a point x_j in the noise cluster is defined to be
$$u_{*j} = 1 - \sum_{i=1}^{C} u_{i,j} \tag{2.1}$$
This algorithm allows noise points to have arbitrarily small membership values in good clusters. Again, the need to correctly specify the value of δ is a drawback of this algorithm.

3. Possibilistic clustering (PC) method [26]. The primary objective of this algorithm is to achieve membership values that are possibilistic i.e. the membership value of a point in a class represents the typicality of the point in the class or the possibility of the point belonging to the class The objective function has a weight factor η which is different for different clusters.

4. The potential function approach [31] and the Mountain method [32, 33]. The potential function approach has been used in automatic pattern classification systems. In this approach the feature points are likened to energy sources. The potential generated by each feature point x_k has a peak value at the location of the feature point and decreases rapidly at any point x away from the feature point. The idea behind the potential function approach can be used to define an objective function to locate clusters. The mountain

method finds the peaks in the potential function. It requires the setting up of a grid in the feature space in order to search for the peaks. This becomes impractical in higher dimensions. The computation of the total potential at a data point is done in which a resolution parameter α is to be specified. Similarly after a cluster is identified, it has to be removed from the data set by discounting the contribution due to the cluster center to the potential at every point using a function in which a resolution parameter β is to be specified. Though this method is quite robust if the clusters are spherical if suitable values of α and β can be found. The main disadvantage of this approach is that the results will be sensitive to the values chosen for α and β.

5. Least biased fuzzy clustering method [34]. This algorithm is based on the deterministic annealing approach and tries to minimize the clustering entropy. The clustering algorithm works by starting with a data point as the initial centroid and then maximizing the clustering entropy and updating the centroid alternately until convergence. Maximizing the entropy again needs a resolution parameter called β . The problems encountered with this algorithm are mentioned further.
   (1) For a given resolution parameter β one would find clusters only of a particular size. (2) The level of computation required is high for this algorithm. (3) The noise sensitivity or robustness aspects of this algorithm are not addressed by the authors.

6. Iteratively reweighted least-squares (IRLS) approach [35, 36, 37]. This method is a popular technique in computer vision and is used to obtain a Robust estimate of parameters starting from a rough initial estimate. The weights are monotonically decreasing functions of the residuals.

7. Robust Competitive Agglomeration(RCA) algorithm [38]. This combines the advantages of hierarchical and partitional clustering techniques RCA determines the "optimum" number of clusters via a process of competitive agglomeration while knowledge about the global shape of clusters is incorporated via the use of prototypes.The survey indicates that RCA is a general purpose algorithm that attempts to achieve robustness with reasonable com-

putational complexity.

2.10 Mean Shift Filter

An interesting non parametric robust technique for segmentation of images is proposed by Comaniciu et al in their papers [72, 73].The authors use a non parametric estimator of density gradient, the mean shift, in the joint, spatial-range (value) domain of gray level and color images for discontinuity preserving filtering and image segmentation. Properties of the mean shift are reviewed and its convergence on lattices is proven. The proposed filtering method associates with each pixel in the image the closest local mode in the density distribution of the joint domain. As this filter forms the basis for the work in the thesis, it is studied in detail in the next chapter.

2.11 The concept of Stochastic Resonance

The term stochastic resonance was coined by Roberto Benzi et al in their seminal paper,"The Mechanism of Stochastic Resonance" [43]. In this paper the authors show that a dynamical system subject to both periodic forcing and random perturbation may show a resonance (peak in the power spectrum) which is absent when either the forcing or the perturbation is absent.

The first direct evidence of SR was reported by Fauve and Heslot [51] in 1983 through their experiments on an ac-driven Schmitt trigger. Later, the paper by McNamara et al [52] on bistable ring lasers led to a series of papers by the Physics community. In [55], stochastic resonance is said to describe a phenomenon that is manifest in nonlinear systems whereby generally feeble input information (such as weak signal) can be amplified and optimized by the assistance of noise. The effect requires three basic ingredients namely a threshold, a weak coherent input and a source of noise. Given these features, the response of the system undergoes resonance-like behavior as a function of the noise level, hence the name stochastic resonance. The authors declare the underlying mechanism as fairly simple and robust. This was a very important input for the research work as it enabled the consideration of Stochastic Resonance as a robust technique for boosting weak signals.

Benzi et al [43, 44, 45] and Nicolis et al [46, 47, 48, 49, 50] propose an explanation of the phenomenon of the ice ages using the concept of SR. The authors show that statistical analysis of variations in the volume of glaciers in the last 10^6 years has a characteristic variation period of 10^5 years. It is pointed out that a possible natural cause that can be correlated with the event and has the same frequency is the modulation of the eccentricity of the earth's orbit due to gravitational perturbation. The intensity of this phenomenon is however too low to be solely responsible for glacier formation. If however the weak exchanges of heat between the sun and the earth's surface are considered to be a further cause of the phenomenon, their interaction with the modulation of the earth's orbit could explain the phenomenon.

Benzi schematises the interaction by means of potential with two wells in which one minimum represents the temperature of the surface covered with ice while the other represents the melting temperature. The slight modulation of the eccentricity of the earth's orbit is represented by a noise with a Gaussian probability distribution. The interaction between these two signals enables the system to oscillate between on state and the other at the same frequency as the periodic signal,thus giving rise to the phenomenon of glacier formation. This interpretation has been given in [53]. The survey on SR concepts gave deep insight into how SR phenomenon actually occurs.

Bulsara and Gammaitoni in their paper on Stochastic Resonance [54]indicate that for a non-linear system having a periodic modulating signal so weak as to be normally undetectable , one of a class of noise-induced coperative phenomena can often be setup leading to a resonance between the weak deterministic signal and the stochastic noise. Such a resonance, in effect matches characteristic deterministic and stochastic time scales making the signal apparent.

In the same paper, the basic SR mechanism is explained by considering a simple system - a bistable dynamical system that can switch between two stable states. The dynamics is characterized by a potential function. The system can be visualized as a marble in a two egg carton. A gentle rocking of the carton will cause the marble to roll back and forth within the one of the egg wells, only under a much stronger disturbance will it surmount the wall and enter the other well. In the absence of any external forcing, friction will cause the system's output(the mar-

ble's position) to settle near the bottom of a well. A more complex output when an external forcing- composed of a deterministic signal(here assumed to be time periodic) and stochastic noise(usually assumed to be Gaussian) is applied. The external forcing may be interpreted as a periodic rocking of the potential while it is simultaneously jiggled randomly by the noise. If the deterministic rocking is too weak to cause the system system to scale the potential barrier in the absence of noise, we call it"sub-threshold". The addition of even small amounts of noise, however can give a finite switching probability to the response, that is some potential barrier crossings will occur. For moderate noise the switchings will acquire a degree of coherence with the underlying signal, the switching probability is briefly maximized whenever the signal is at its own maximum. The barrier crossing rate thus depends critically on the noise intensity. If the noise intensity is very low, the probability of any switching occurring at all is tiny. On the other hand, intense noise can induce switching even during an "unfavorable interval" when the signal is close to its minimum, the signal will be swamped. In between one expects to find a range of noise intensities that induce switching events in near-synchrony with the signal.The authors mention that this corresponds to some form of resonant behavior in the dynamics.

2.12 Application of SR in other domains

Gammaitoni et al in their paper [55] report, interpret and extend the understanding of the theory and physics of stochastic resonance. Definitions of the characteristic quantities that are important to quantify stochastic resonance together with the tools necessary to compute these quantities are presented.

Francois Chapeau-Blondeau [56] demonstrates that a nonlinear detector can act as an SNR amplifier delivering an output SNR larger than the input SNR. Further, it is indicated that if the threshold θ is an adjustable parameter, then it can be set to an optimal value which depends upon the properties of the input signal-plus-noise mixture. This optimal value for θ at the same time maximizes the output SNR and the input-output SNR gain. The author further indicates that when the detector has to operate at a fixed threshold $\theta > 1$, there exists an optimal nonzero input noise level that maximizes the output SNR.

Donatella Petracchi et al [57] discuss the relevance of SR in biological systems.

The paper reviews the conference on "SR in biological systems" and highlights that SR can occur by transmission and amplification in living organisms by enzymatic cascades or by taking advantage of the energy stored in the electrochemical gradient through the cell membrane. The conclusion is that work on SR in biological systems will be very beneficial.

Donatella Petracchi [58], defines SR as an "improvement of signal transmission by increasing the input noise up to an optimal value in systems whose stochastic switching from one state to another is modulated (but not directly determined) by an applied perturbation". The paper discusses the role of SR in detection of signals.

Z. Gingl et al [59] show that SNR gains larger than one can be provided by one of the simplest bistable stochastic resonator system, a Schmitt-Trigger. The results indicate that SNR gain requires only two conditions: spiky signal and nonlinear response limit. The authors conclude by mentioning that spiky signals are good for demonstrating SR.

The case for use of SR as a robust technique in image processing comes from the paper by Steeve Zozor et al [60] in which the authors build a detector that uses SR phenomena in spite of a lack of knowledge of the noise pdf or of the noise σ.

The use of SR in the stock market is given in the paper by Peter Babinec [61] wherein the author show that an increase in the noise (market volatility) increases the SNR describing the response to the global periodic investment bias.

Another interesting paper by Bohou Xu et al [62] demonstrates the SR effect by tuning system parameters instead of tuning noise levels,since the latter is sometimes not possible. The authors mention that when the noise intensity sweeps over the optimal operating point or resonance region, the conventional method of SR via tuning noise cannot obtain the maximum value of the output SNR. This has led to an important concept in our Stochastic Bucket algorithm (discussed subsequently) wherein bucket sizes are changed.

In the paper by Aditya A. Saha et al [63] it is shown in the context of signal processing in ocean acoustics that the signal detection performance of an SR based detector is better than that of the matched filter for a large class of noise distributions that belong to the generalized Gaussian and mixture-of-Gaussian

families.

Bart Koskoa et al [64] in their paper on SR in noisy threshold neurons, show that small amounts of independent additive noise can increase the mutual information of threshold neurons if the neurons detect sub-threshold signals. The authors' second theorem shows that SR effect is robust against violent fluctuations in the additive noise process. This has been a strong reason for considering SR in image processing in our research.

Hu Niaoqing et al [65] apply SR in the early detection and prediction of rub-impact faults in rotors of rotating machinery. SR is applied to real-time application and it is indicated that it is suitable for detecting weak useful signals in heavy noise from short data records. The advantages of SR for mechanical fault diagnosis are proven.

The investigation of SR phenomena in chemical reactions is explored in the paper by Fan Zhang et al [66].

Ashok Patel et al in their paper [67] show that small amounts of additive white noise can improve the bit count or mutual information of models of spiking retinal neurons and spiking sensory neurons. Possibility of benefit from noise injection in artificial retinas, neural prosthetics, low-light imaging and night vision, IR imaging and object detection is mentioned.

An interesting paper by Barney E. Klamecki [68] on the use of SR for enhancing low level signals mentions the advantages of the technique in the promotion of a signal that is below the system noise level to a useful level above the system and ambient noise levels. The advantage of improvement in SNR with added noise level for a vibration signal for a mechanical system having a worn bearing is demonstrated. The utility of SR in improving the performance of different optimal detectors like Bayesian, minimum error-probability, Neyman-Pearson and minimax detectors is demonstrated by David Rousseau and Franois Chapeau-Blondeau in their paper [69].

Yong-gang Lenga et al [70] in their paper give two examples of detecting a weak signal embedded in strong noise are presented to illustrate that a single bistable system and a cascaded bistable system are both powerful tools for signal processing.

Another interesting application of SR is in the domain of target detection

in shallow-water reverberation by Bohou Xua et al [71] wherein spatial signals interfered by Gaussian noise are effectively recovered.

The following papers which have appeared in the final stages of the research work have given additional insights into SR and its futuristic research like considering multi-scale noise for noise injection and also for applying the work for non-Gaussian noise.

D.W. Repperger et al [90] use nonlinear control theory analysis to better understand the class of systems that may exhibit the SR effect. Using nonlinear control theory methods,equilibrium points are manipulated to create the SR response (similar to shaping dynamical response in a phase plane). From this approach, a means of synthesizing and designing the appropriate class of nonlinear systems is introduced. New types of nonlinear dynamics that demonstrate the SR effects are discovered, which may have utility in control theory as well as in many diverse applications.

The application of SR to feature extraction for low quality fingerprint images is demonstrated by Choonwoo Ryu et al [91]. Experimental results in this paper show that Gaussian noise added to low quality fingerprint images enables the extraction of useful features for biometric identification.

Qingbo He et al in their paper [92] show that the weak signal can be effectively detected from heavy background noise via the SR phenomenon by tuning multi-scale noise. The authors conclude that : (a) under the new strategy, the SR phenomenon can appear at different noise intensity with a same tuning parameter (b) the multi-scale noise with a corresponding analysis scale has shown to be an active role in detecting weak signals (c) the proposed SR model has shown good capability in detecting a wide range of driving frequencies. Therefore, the proposed new strategy has shown the potential in general application to detect weak signals with a wide range of frequencies at any given noise intensity. Bearing defect identification by using weak signal analysis is confirms its effectiveness.The applicability for noise handling in image processing gets strengthened by this paper.

Qingbo He et al [93]further propose an SR approach which over comes the limitation of small parameter requirement of the classical SR and takes advantage of the multi-scale noise for an improved SR performance. Thus the method is well-

suited for enhancement of rotating machine fault identification when the noise is present at different scales.

The design and performance analysis of a detector based on supra-threshold stochastic resonance (SSR) for the detection of deterministic signals in heavy-tailed non-Gaussian noise is presented in the paper by V.N. Hari et al [94].

2.13 SR in Image Processing

The enhancement of images using stochastic resonance and application to sonar image processing is discussed in [81]. The application of SR to improve the quality of the noisy input image to get the de-noised response image is shown in [82]. Input noisy image is subjected to independent additive white Gaussian noise of different standard deviation, the output image corresponding to individual noise standard deviation, summed and averaged, to get the de-noised image. This paper gives a useful insight on the application of SR to image de-noising without going into mathematical analysis of the improvement of PSNR during the process. Clearly, a strong case may be made out for carrying out such an analysis.

2.14 Classification of Images

In order to evaluate the segmentation performance of different techniques mentioned above on noisy images, a need to classify images was felt. This would be useful in identifying the merits and demerits and their suitability for a particular class of image. The candidate images for segmentation can be classified into four types namely :

- High SNR images having a strong signal and a weak noise component.
- Medium SNR Images in which signal and noise were both strong.
- Low SNR Images in which signal and noise were both equally weak.
- Very low SNR images in which the signal is relatively weaker (due to small features and/or low amplitude) compared to the noise in the image.

Weak signals images can be categorized into two types. (i)Those in which features are small in size and (ii)Those in which features are small in amplitude. The next

section compares the different techniques surveyed and their applicability to these four categories of images.

2.15 Comparison of the techniques from Statistics and Computer Vision

A study of the techniques from statistics, computer vision, clustering, non parametric estimation domain and unconventional techniques like stochastic resonance revealed the following observations.

- All robust techniques from statistics and computer vision perform well with high SNR images.
- While LMS and M-estimators (from statistics) need to estimate the scale, Hough transform and RANSAC (from computer vision) treat scale as a tuning constant. In the presence of strong noise in the image, it is difficult to estimate the scale in techniques from computer vision. Hence the techniques give degraded performance for medium SNR and low SNR images
- All these techniques fail for the very low SNR images when the discontinuity magnitude is 7.5σ or more.The failure appears in the form of a surface that bridges two actual surfaces.
- In techniques from robust statistics, weight functions define the resistance to outliers.In the presence of strong noise and weak signal due to small features located close to each other, the clarity between outliers and inliers may be lost. Hence these techniques will fail in very low SNR images.
- In the presence of strong noise, additional overlapping surfaces can appear. The MINPRAN is capable of estimating patches which are overlapping with a criteria for the number of points contributing to the patch. Thus it can handle medium SNR images considering the noise strength in these images will match the signal strength.
- Images with weak signals in which features are small in size are handled better by MUSE and ALKS with the condition that the magnitude of the

discontinuity between nearby surfaces is less than 4.5σ where σ is the standard deviation of the noise. Thus these techniques can handle medium SNR images to the extent that this criteria is met.

- For clustering techniques the cluster validity plays an important role in robust clustering without which it is not possible to identify the clean pixels from the noisy pixels and the outliers in an image.These techniques are not efficient when the number of clusters are not known. The study indicates the applicability of these techniques only to the medium SNR image category.

- Non parametric estimation techniques like the mean shift filter depend on two normalization constants, σ_s and σ_r for filtering low SNR images. Since kernel density estimation is used there is no need to estimate the underlying density function. However the performance depends on the values chosen for these constants which are again subjective to the test image. The resistance to outliers for these techniques is not clear from the survey.

- Techniques like stochastic resonance which inherently boost the weak signals are likely to handle better the low SNR category images and the papers on application of SR indicate strong reasons favoring the same.

2.16 Conclusions

The survey of the different algorithms for segmentation of noisy images has given significant inputs for the research work. These are summarized below.

- The survey of the various robust techniques from statistics, computer vision and clustering approaches has indicated that these techniques attempt to perform robustly in the presence of noisy data and outliers. In practice, there are several problems like specifying the scale especially when scale is a function of noise. Other problems include multiple surfaces, bridging fits , unknown clusters, cluster validity and appropriately specifying resolution parameters to the algorithms.

- These robust techniques are suited for segmenting images of category I and category II. For the second category, the performance degrades with noise.

However, the survey does not give inputs on how the performance degrades with increasing noise and the limits of these robust techniques in handling noise. For category III images, these algorithms tend to remove features.

- These techniques cannot handle images of category III where the signal is weak due to either small-sized features or small-amplitude features because of the need for specifying scale, cluster validity related issues etc. Since stochastic resonance has been able to handle weak signals by boosting them in the presence of noise in other engineering domains, the survey clearly points towards the possibility of its use in category III images. However, the limits of SR in such applications is not clear from the survey.

- Non parametric estimation techniques appear to be the best candidates for further research on robust techniques since a priori knowledge of the underlying density function is not required. The mean shift filter which is a mode seeking filter has been found quite effective [72, 73] for segmentation of clean images. However, its performance in the presence of noise is not clear.

- Most significantly, none of the available techniques can handle the category IV images which are very low SNR images in which the signal is far weaker than the noise. Research on robust segmentation of low SNR images has been aimed at high noise cases but not on images having weak signals.

- Clearly,there is a need for research on algorithms for segmentation of images of category IV type.

- The survey clearly indicated that Robust Techniques and Stochastic Resonance were two different approaches - the former for reducing the noise and the latter for boosting the signal. The survey indicated that no research has been done till now for bridging the gap between these two approaches and clearly the possibility of integrating these two complimentary approaches which can handle images with high amount of noise even better existed.

The above major conclusions has lead to research on algorithms for handling the category IV images. Such images were important in images where the fine features need to be detected for the desired application. The subsequent chapters are closely linked to these conclusions. In Chapter 3, the mean shift filter as

a representative algorithm of non-parametric estimation techniques is studied in detail for its tolerance to noise in low SNR images. The performance limits in the presence of noise are obtained for the algorithm. In Chapter 4, variants of this algorithm are developed to overcome its limitations in the present form and the performance of these variant algorithms in the presence of noise are studied. The ability of Stochastic Resonance to boost weak signals especially the edge pixels is studied in the research work presented in Chapter 5. Also the development of a new paradigm for handling category IV images and its performance is presented in this chapter.

Chapter 3

Mean Shift Filter and its Characteristics

3.1 Introduction to Non-parametric Techniques

In parametric techniques, the general form of the probability distribution function or density function for the available data can be assumed. However, in most real problems like those in computer vision and image processing, the types of density functions are unknown and it is not easy to identify which density function could be used. The non-parametric technique is most suitable for such situations. In this technique arbitrary density functions are fit to a set of samples. For example, the histogram approximation of an unknown pdf is a non-parametric approach. As mentioned in [73] a feature space is a mapping of the input obtained through the processing of the data in small subsets at a time. For each subset, a parametric representation of the feature of interest is obtained and the result is mapped into a point in the multi-dimensional space of the parameter. After the entire input is processed, significant features correspond to denser regions in the feature space i.e to clusters and the goal of the analysis is the delineation of these clusters. Images can be represented by arbitrarily structured feature spaces. In the context of image processing non-parametric methods are classified as

1. Hierarchical clustering methods.

2. Density estimation methods.

Hierarchical clustering techniques either aggregate or divide the data based on some proximity measures. These techniques have already been covered in the previous chapter. It may be noted that these techniques are computationally expensive and the stopping criterion for fusion is not straightforward. In kernel density estimation techniques, the feature space can be regarded as the empirical probability density function of the represented parameter. Dense regions in the feature space correspond to local maxima of the probability density function, i.e to the modes of the unknown density. Once the mode is located [74, 75, 76], the cluster associated with it is delineated based on the local structure of the feature space.

3.2 Kernel estimators

The concept of kernel estimators is explained in [30].The samples in the image dataset can be thought as a very rough approximation to the true density function. The sample can be represented as a set of spikes or delta functions, one at each sample value, each with a very small width and a very large height such that the combined area of all the spikes is '1'. The area of each spike is the number of samples lying at that point divided by the total number of samples. If the delta functions at each sample point are replaced by other functions called *kernels* such as rectangles, triangles or normal density functions which have been scaled so that their combined area equals one then their sum produces a smoother, more satisfactory estimate. There are several types of kernels like rectangular, triangular, normal and Epanechnikov kernels. Estimates of density functions in n dimensions $p(x)$ where x is an n-dimensional vector are obtained as sums of n-dimensional kernels centered at the samples normalized so that their total hyper volume or probability equals 1.

An important issue with kernel estimation is choosing good widths or standard deviations. If the width is too large, fine structure will be lost but if the width is too small, the resulting approximation will not be sufficiently smooth but will contain noisy fine structures due to the random locations of the samples. The width or the standard deviation of the window should be sufficiently large so that several samples will fall within this range on the average. In practice several different widths are usually tried and the best is chosen intuitively, according to prior

knowledge or according to its classification performance on the training data of interest. As the number of samples within the window approaches infinity and the window width itself approaches zero, the estimated density function will approach the true density for any reasonably well-behaved window function. The properties of the kernel is very significant in estimating the density. A triangular kernel, for example, is not differentiable at all points and so its slope has discontinuities. The normal kernel is on the other hand, infinitely differentiable. In the former case the estimated density is "rougher" than that obtained from the later kernel. To emphasize, the shape and properties of kernel functions help to better understand the density function underlying a given set of data.

Kernel density estimation techniques(also called as Parzen estimation) have the potential for being applied to noisy images. The density estimation can lead to the discovery of peaks and valleys in the data set. This research work is based on the premise that kernel techniques when correctly applied can enable discrimination of the inliers from the outliers by way of identifying the peaks resulting from the inliers.

3.3 Multi-dimensional kernel density estimation

If $\{x_i\}_{i=1\cdots n}$ is an arbitrary set of n points in the d-dimensional Euclidean space R^d, then the multi-variate kernel density estimate that is obtained with kernel $k(x)$ and window radius h, computed at point x is defined as

$$\hat{f}(x) = \frac{1}{nh^d} \sum_{i=1}^{n} k(\frac{x - x_i}{h}) \tag{3.1}$$

The role played by h in the above equation is important [77]. When the value of h is small a lot of noise or spurious structure is obtained in the estimate. With a larger value a smoother estimate is obtained but there is a possibility that bumps or other interesting structure may get obscured in the estimate. In practice, it is recommended that the analyst examine kernel density estimates for different window widths to explore the data and to search for structures such as modes or bumps. The value of h should be chosen so as to minimize the asymptotic mean integrated square error (AMISE). The choice of smoothing parameter h , is more important than choosing the kernel. This arises from the fact that the effects from the choice of kernel (e.g kernel tail behavior) are reduced by the averaging process.

Table 3.1: Examples of kernels used in density estimation

S.No.	kernel name	Equation
1	TRIANGLE	$k(t) = (1 - \|t\|) \quad -1 \leq t \leq 1$
2	BIWEIGHT	$k(t) = \frac{15}{16}(1 - t^2)^2 \quad -1 \leq t \leq 1$
3	TRIWEIGHT	$k(t) = \frac{35}{32}(1 - t^2)^3 \quad -1 \leq t \leq 1$
4	NORMAL	$k(t) = \frac{1}{\sqrt{2\pi}} * e^{-t^2/2} \quad -\infty < t < \infty$
5	EPANECHNIKOV	$k(t) = \frac{3}{4}(1 - t^2) \quad -1 \leq t \leq 1$

What is important in the choice of a kernel are computational considerations or the amount of differentiability required in the estimate.

Examples of some of the kernels used for density estimation are mentioned in [**?**] and given in Table 3.1. In terms of efficiency, the optimal kernel was shown to be the Epanechnikov kernel [78]. The other choices for kernel are indicated in the above table. In [79] and [80] it is shown that these kernels have efficiencies close to that of the Epanechnikov kernel, the least efficient being the normal kernel.

3.4 Mean shift analysis

When the Epanechnikov kernel is used for the function k above, we get the minimum value for the mean integrated square error (MISE). If the kernel is differentiable then the estimate of the density gradient is the gradient of the kernel density estimate

$$\hat{\nabla} \equiv \nabla \hat{f}(x) = \frac{1}{nh^d} \sum_{i=1}^{n} \nabla k(\frac{x - x_i}{h}) \tag{3.2}$$

For the Epanechnikov kernel, the density gradient estimate becomes

$$\hat{\nabla} f(x) = \frac{1}{n(h^d c_d)} \frac{d+2}{h^2} \sum_{x_i \in S_h(x)} (x_i - x) \tag{3.3}$$

$$\hat{\nabla} f(x) = \frac{n_x}{n(h^d c_d)} \frac{d+2}{h^2} (\frac{1}{n_x} \sum_{x_i \in S_h(x)} (x_i - x)) \tag{3.4}$$

Where $(\frac{1}{n_x} \sum_{x_i \in S_h(x)} [x_i - x])$ is the sample mean-shift and $S_h(x)$ is a hyper sphere of radius h having the volume $h^d c_d$, centered on x and containing n_x data points.

$$\hat{\nabla} f(x) = \frac{n_x}{n(h^d c_d)} \frac{d+2}{h^2} M_h(x) \tag{3.5}$$

$$\hat{\nabla} f(x) = \hat{f}(x) \frac{d+2}{h^2} M_h(x) \tag{3.6}$$

$$M_h(x) = \frac{h^2}{d+2} \frac{\hat{\nabla} f(x)}{\hat{f}(x)} \tag{3.7}$$

Equation (7) shows that an estimate of the gradient (normalized) is obtained by computing the sample mean shift in a uniform kernel centered on x. The mean shift vector has the direction of the gradient of the density estimate at x when the Epanechnikov kernel is used. The successive application of mean shift defines a path, which leads to the local density maximum [72, 73]. In the mean shift filtered output, all the points that lie on the path are assigned local density maximum as their values. When applied to an image, the image is represented as a 2D lattice of one- dimensional vectors for gray scale and three-dimensional vectors for color images. The pixel information is normalized with two constants: σ_s in the spatial domain, and σ_r in the range domain. These two constants subdivide the space containing the image data (x and y spatial coordinates and z values) into cuboids of dimensions σ_s along the x and y directions, and σ_r along the z direction. The cuboids are called *buckets* in [72] and we use the same notation here. Mean shift is calculated using only the pixels present in neighboring buckets and the pixels may be weighted according to the bucket in which they are present. The size of the neighborhood and the weights are given by the kernel functions $k(x)$. For the Epanechnikov kernel used in [72], 27 buckets 3x3x3 surrounding the bucket containing the pixel under consideration are used in estimating the kernel density gradients and hence the mean shifts. All the buckets are weighted equally. Figure 3.1 shows the concept of the image getting transformed into the three-dimensional spatial-range data. The bucket size is decided by the value chosen for σ_s and σ_r. Therefore, all the buckets have the same size in the x and y direction (based on the value chosen for σ_s). Similarly, the buckets have the same size in the z direction (based on the value chosen for σ_r).

The choice of values for these two constants is by no means straightforward. As mentioned in [72], these two constants are related to the spatial and range resolutions of the image, noise parameters and models, and need incorporation of

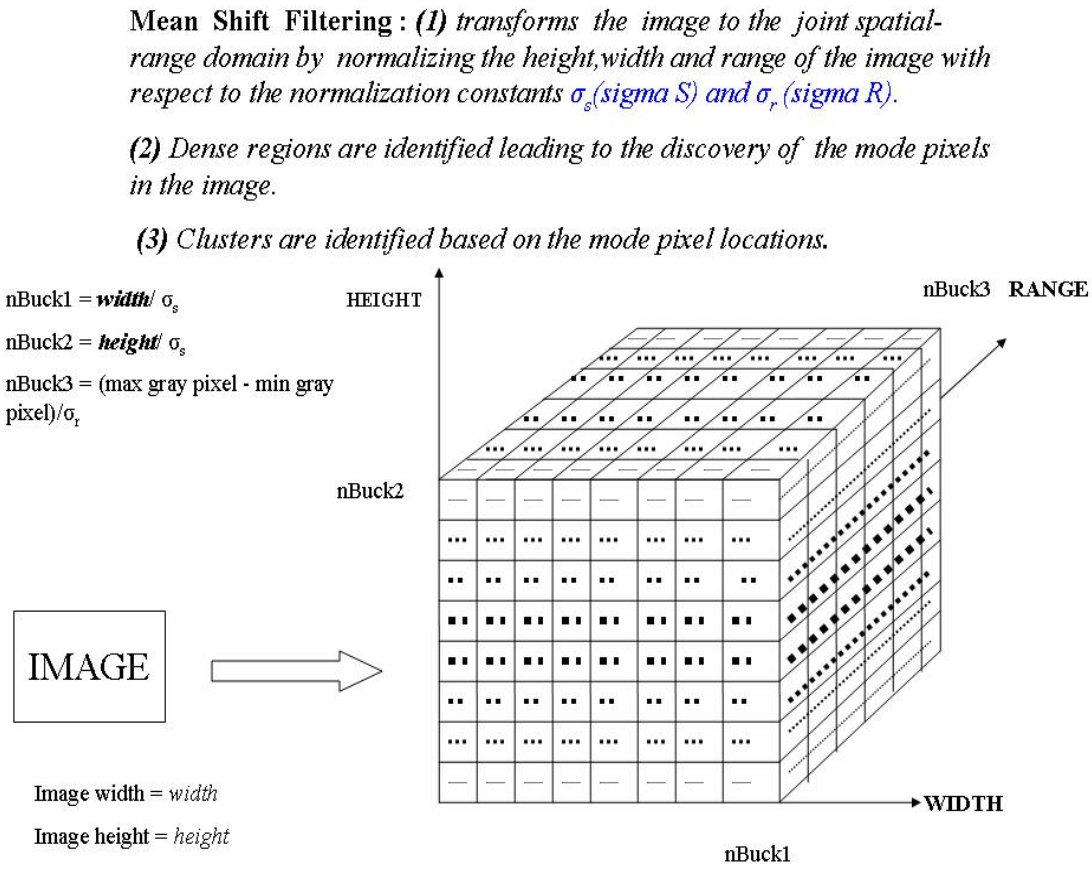

Figure 3.1: The transformation of the image data into the three-dimensional spatial-range data in the three-dimensional space and the allotment of the pixels to the respective buckets. The number of buckets in each axis are determined by the image dimensions and the values of σ_s(sigma S) and σ_r (sigma R) in the spatial dimensions and the range dimensions respectively

top-down knowledge-driven approach for their selection.
In [72] the authors show that the mean shift filtering technique is effective in carrying out segmentation of clean images. Our research was focused on studying the mean shift analysis technique, analyzing the effect of noisy pixels and bucket sizes on the filtering effectiveness and confirming the same by application to images corrupted with Gaussian noise.

3.5 Experiments on mean shift filtering

As part of the research work we designed a number of experiments that ranged from using fixed-size buckets with different values of σ_s and σ_r to using variable-size

buckets that adapt their dimensions to the local properties of an image. The main idea was to study and understand the effect of these two normalization constants, how noise affects their selection and whether there is a method to predetermine the best values from either knowledge of the application domain or estimation from the images themselves. In this chapter, we report the studies on fixed size buckets. The work on variable sized buckets is discussed in the next chapter.

3.6 Analysis of bucket size effects

A qualitative analysis of the size of buckets let us hypothesize the following for images corrupted with Gaussian noise.

1. A small value of σ_s will restrict the computation of mean shift to those in the immediate neighborhood of a pixel in consideration. Choosing too small a value may result in a biased estimate of the mean-shift vector.

2. A large value of σ_s will make the buckets large in the spatial dimensions, i.e., the neighborhood under consideration becomes large. As the mean shift vector is computed from a larger neighborhood, it results in an unbiased estimate, but the spatial resolution is the casualty. It leads to blurring and loss of fine details in the image.

3. A small value of σ_r will restrict the variation in intensities in a given spatial region and thus may work well only on images containing largely uniform regions. On other types of images, it may lead to over segmentation.

4. A large value of σ_r has the opposite effect of permitting a greater variation in intensities in the neighborhood and may result in under-segmentation.

5. In the presence of noise, a small value for σ_r can potentially confine noise values to buckets that are outside the neighborhood and thus improve performance. Similarly, a larger value of σ_s leads to a behavior analogous to using an averaging kernel of a large size.

An experiment was carried out for evaluating the performance of the Mean Shift filter.In this experiment, different amounts of Gaussian noise was added to test images. The filtered outputs were quantitatively evaluated for various values of σ_s and σ_r using the following three measures.

1. Peak Signal-to-Noise Ratio (PSNR).

2. Region Count obtained by counting the regions obtained after segmentation of the filtered output.

3. Pratts figure-of-merit to measure the quality of the edges obtained from the segmented image vis-a-vis the Canny edge detector.

3.7 Test Image Database

For testing the various filtering algorithms in the research work a test image database of 160 images was created from 40 images to each of which Gaussian noise of mean $\mu = 0$ and standard deviation σ of 10%, 20% and 30% was added. The noisy versions of the clean images were generated using the imnoise() function available in MATLAB. The image database consisted of standard images (like cameraman, boat, peppers, Lena, Barbara, Flinstones), images of natural objects and landscapes, images of man-made objects, images from space missions and texture images (from the Brodatz texture image database). Thus a database of 160 images consisting of 40 original images and 120 noisy images was created to carry out experiments. The images for the test database were chosen such that most features seen in practical images like edges, corners, shapes, regions and textures were covered. This test database is a comprehensive set of images and is available in the School of Computers and Information Sciences, University of Hyderabad for use by other researchers. Figure 3.2 shows a few samples of this database.

3.8 Experiments on images

The boat, cameraman, peppers and the Lena image were initially used to evaluate the performance of the mean shift filter with clean images and images corrupted with Gaussian noise (σ of 10% and 20%). The mean shift filter algorithm (as implemented by Cominiciu et al) was applied to the four benchmark images and their noisy versions. Refer to Figure 3.3, Figure 3.4, Figure 3.5 and Figure 3.6 respectively.

1. For each image and its noisy versions, the filter algorithm was executed

Figure 3.2: Sample images from the test image database used for the experiments in the thesis

repeatedly with the value of σ_s varying from 1 to 8 and the value of σ_r varying from 1 to 32 (both in powers of 2).

2. Each filtered output was quantitatively evaluated by calculating its peak signal-to-noise ratio (PSNR) with respect to its clean image.

3. For each image, the filtered output with the highest PSNR value (corresponding to a particular combination of σ_s and σ_r) was used to obtain the number of regions found after segmentation.

4. The segmented outputs were subjected to edge detection using the Sobel edge detector. The quality of the edges was measured by using Pratt's figure-of-merit by comparing with the output of the Sobel edge detector (applied to the clean image).

The initial experiments with the four sample images and the noise corrupted versions indicated the presence of a particular combination of σ_s and σ_r which gives the best quality filtered output measured by PSNR. To substantiate the existence of an optimal σ_s and σ_r for every image, 120 images consisting of 40 clean images and 80 noisy images For each of the 120 images, the true edges were detected from the clean image using the Sobel edge detector. The algorithm was executed on all three types of each image to record the PSNR value for different values of σ_s and σ_r. As mentioned earlier the filtered image was segmented and the number of regions were counted. Further, the segmented images were subjected to edge detection. The quality of the detected edges was measured using the Pratts figure-of-merit using the ground truth edge image (obtained from the clean image). These 40 images have been categorized into four categories based on the number of regions (low or high) and on the intensity variation(low or high). Table 3.2 shows the number of images in each category.

3.9 Results

The results that follow in this and subsequent chapters are shown raw as they are. They are not post-processed, as the goal of this thesis is to analyze the weak features.The segmented and edge detected outputs for Gaussian contaminated images of boat, Cameraman, peppers and Lena images are shown in Figure 3.3 to

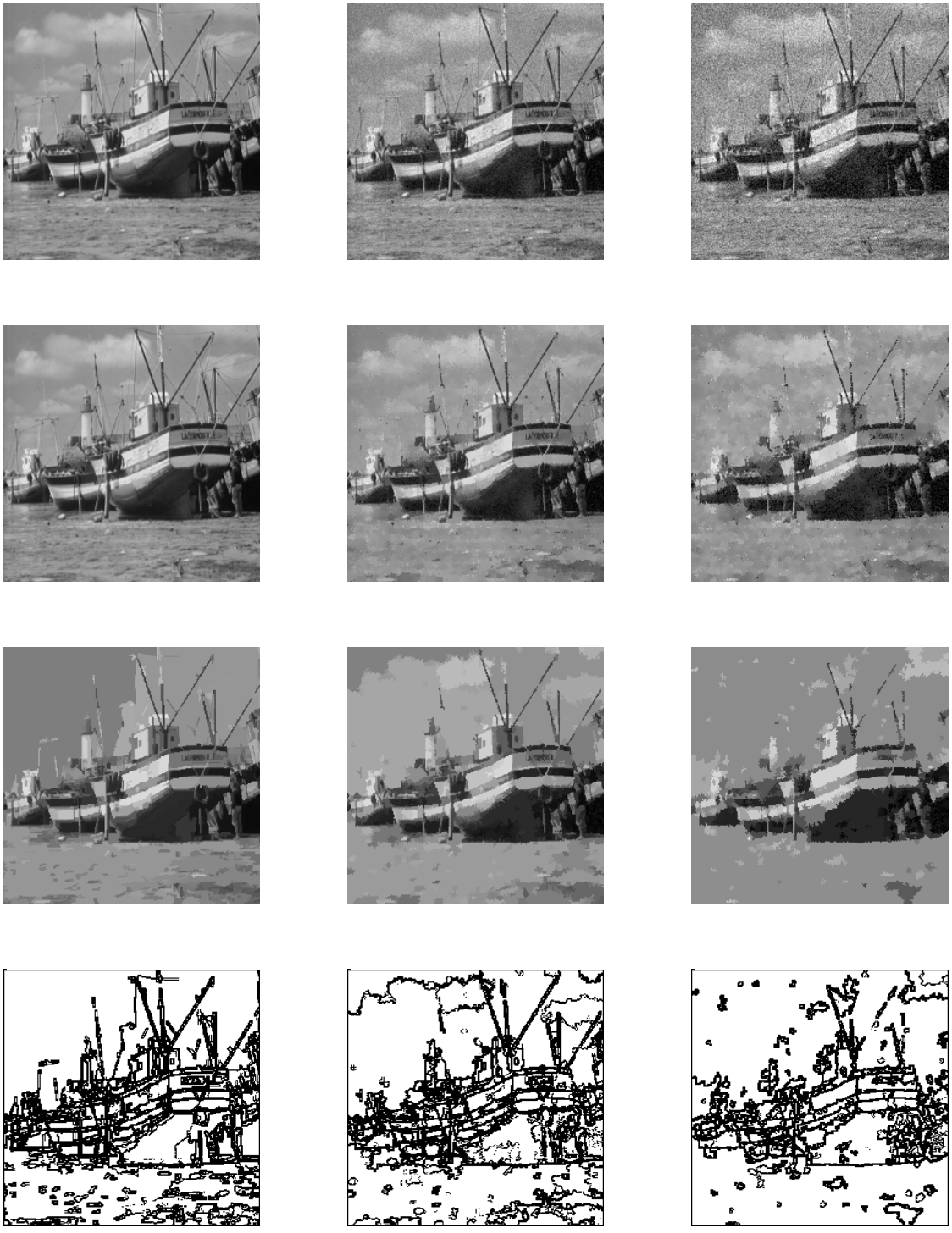

Figure 3.3: Comparative performance of mean shift filter on boat image image without noise (first column), with 10% noise (second column) and 20% noise(third column). The input image is in the first row, the filtered output is in the second row, the segmented output in the third row and the edge image in the fourth row.

Figure 3.4: Comparative performance of mean shift filter on cameraman image without noise (first column), with 10% noise(second column) and 20% noise (third column). The input image is in the first row, the filtered output is in the second row, the segmented output in the third row and the edge image in the fourth row.

Figure 3.5: Comparative performance of mean shift filter on peppers image without noise (first column), with 10% noise (second column) and 20% noise (third column). The filtered outputs are in the second row, the segmented outputs in the third row and the edges in the fourth row.

Figure 3.6: Comparative performance of mean shift filter on Lena image without noise (first column), with 10% noise (second column) and 20% noise (third column). The filtered outputs are in the second row, the segmented outputs in the third row and the edges in the fourth row.

Table 3.2: Image types and numbers

Image Type	Intensity Variation(Low)	Intensity Variation(High)
Region Count (Low)	7	6
Region Count (High)	12	15

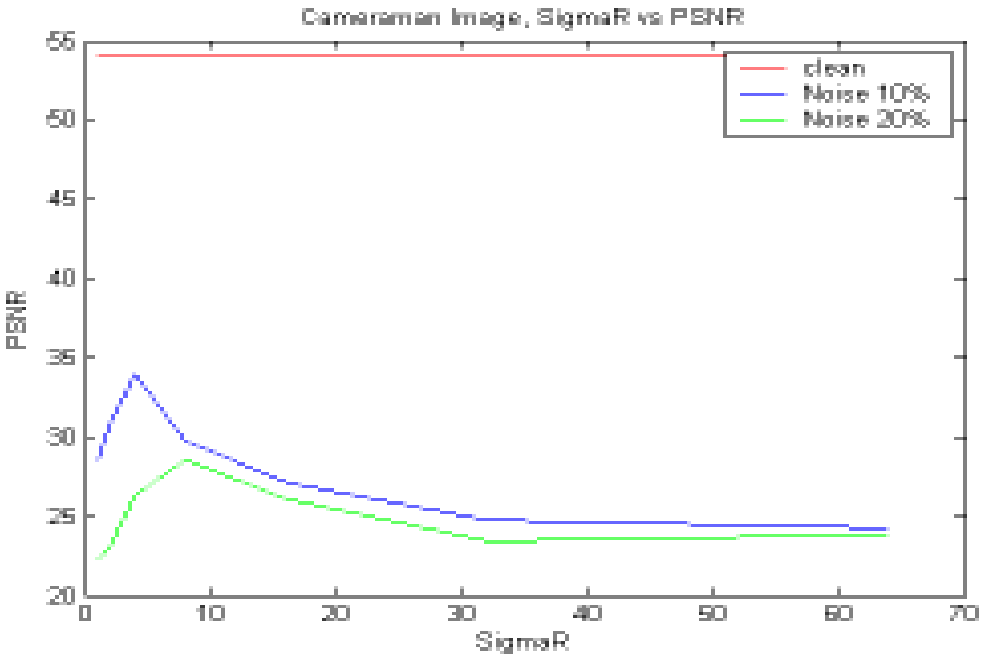

Figure 3.7: The variation of PSNR with σ_r for the cameraman image with 10% and 20% Gaussian noise for a constant σ_s. The curves show a distinct peaking for a certain value of σ_r.

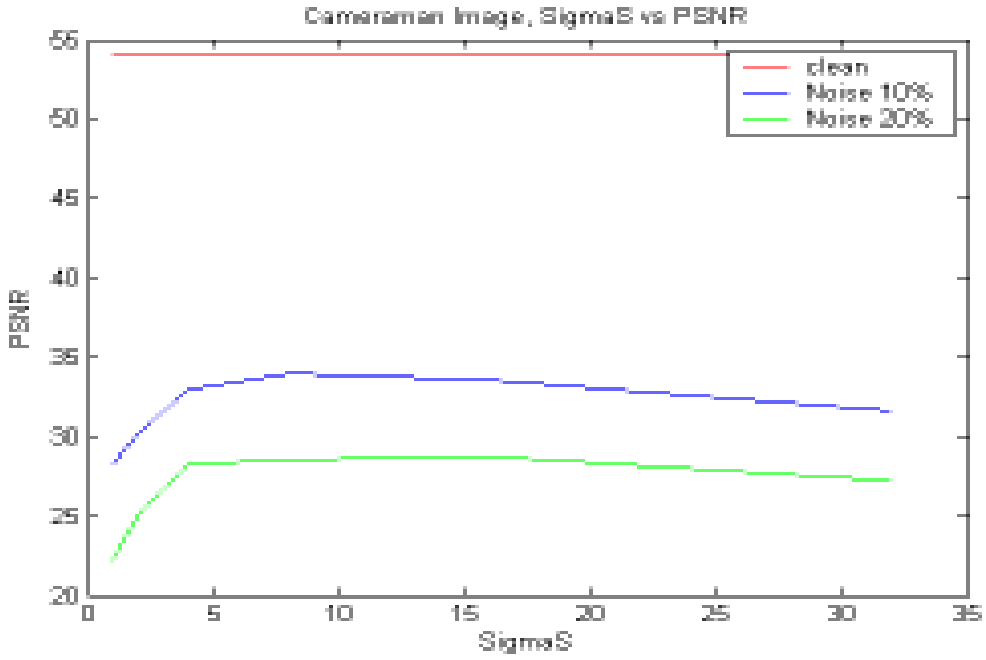

Figure 3.8: The variation of PSNR with σ_s for the cameraman image with 10% and 20% Gaussian noise for a constant σ_r. The curves show a region in which the PSNR is maximized.

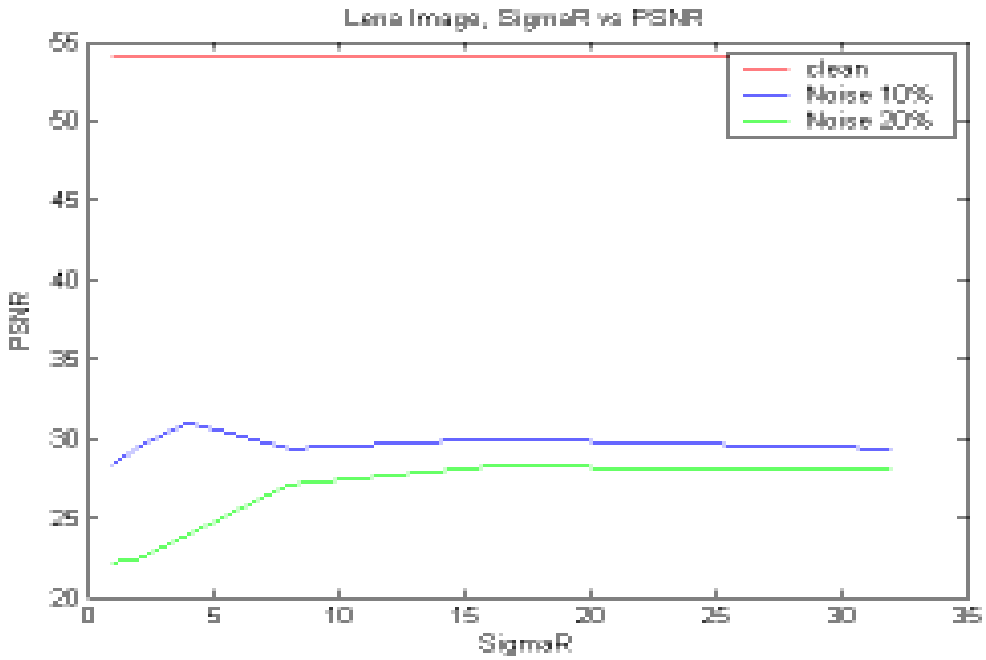

Figure 3.9: The variation of PSNR with σ_r for the Lena image with 10% and 20% Gaussian noise for a constant σ_s. The peaking is more pronounced for the 10% noise case.

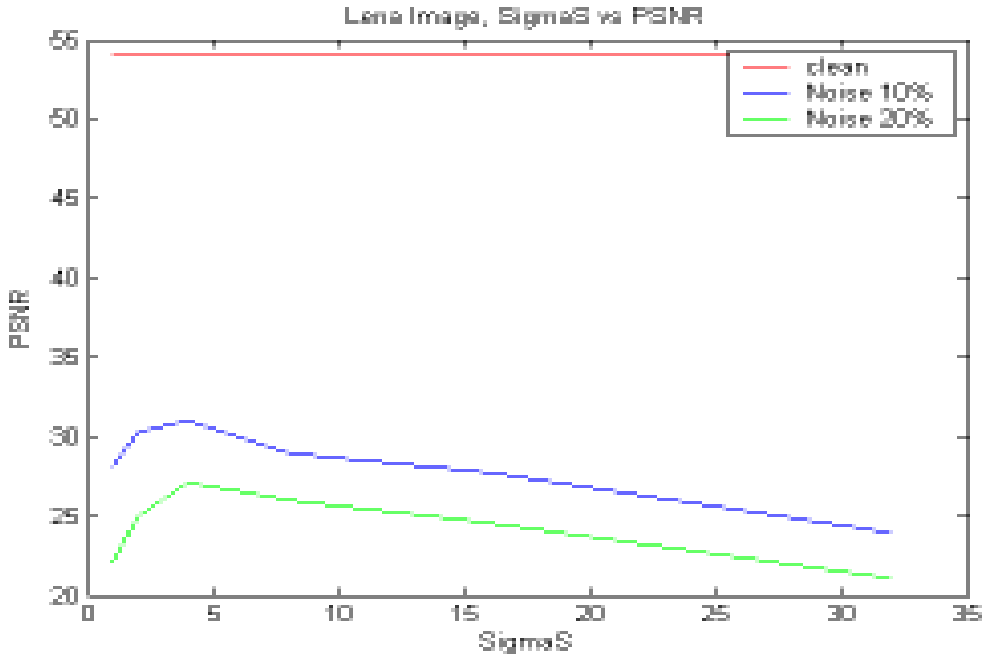

Figure 3.10: The variation of PSNR with σ_s for the Lena image with 10% and 20% Gaussian noise for a constant σ_r. The again curves show a region in which the PSNR is maximized.

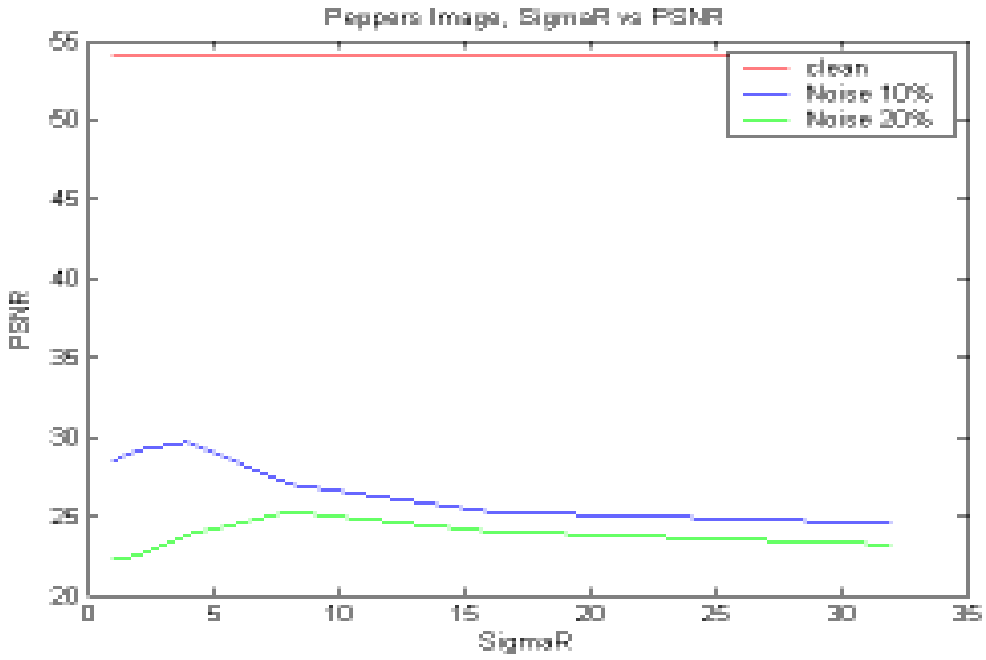

Figure 3.11: The variation of PSNR with σ_r for the peppers image with 10% and 20% Gaussian noise for a constant σ_s. Here the peaking is more pronounced for the 10% noise case.

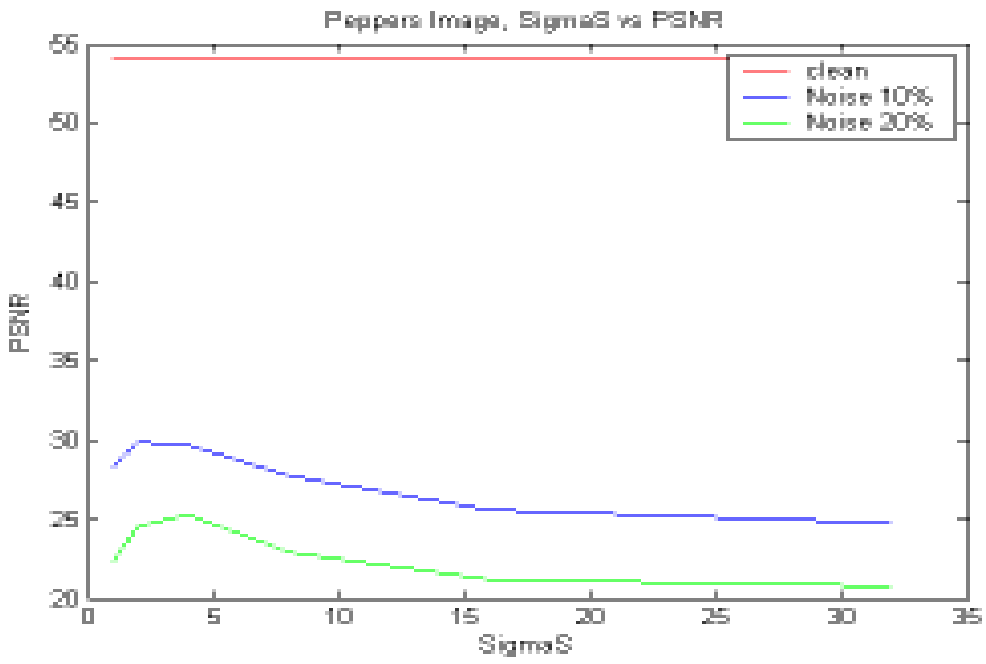

Figure 3.12: The variation of PSNR with σ_s for the peppers image with 10% and 20% Gaussian noise for a constant σ_r. Here the peaking is more pronounced for both cases.

Figure 3.6 respectively. These outputs are for the best values of σ_s and σ_r. It may be noted that the significant features are preserved in the segmented and edge detected outputs for the 20% noise cases in all three images. The quantitative assessment of the filter performance with noisy images is provided by the plots shown in Figure 3.7 to Figure 3.12. In these figures the variation of PSNR with σ_r for a constant σ_s and the variation of PSNR with σ_s for a constant σ_r is indicated. The existence of a peak PSNR for a certain combination of σ_r and σ_s is seen in these figures. This peaking of PSNR results because increasing the σ_s value increases the bucket dimension in the spatial dimension. This causes more number of pixels to enter the bucket resulting in a more unbiased estimate of the mean shift vector. Further increase in value of this parameter causes pixels from other segments/features in the image to enter the estimate leading to less correct estimates of the mean shift. This behavior is observed for all the images.

The effect of σ_r on PSNR for Gaussian corrupted image is also found to be similar for all three test images. For a given value of σ_s, increasing the value of σ_r causes more pixels to enter the estimate of the mean shift vector. More number of pixels will make the estimate more unbiased until a certain point where noisy and

outlier pixels start entering the buckets and the PSNR value starts decreasing. The detailed results for all the 40 images and the contaminated versions with 10% and 20% Gaussian noise are given in the Appendix. The following points summarize the results of the experiments.

1. The mean shift algorithm gives the best output (highest PSNR) for a σ_s and σ_r value of 1 for clean images. This means that a bucket size of 1 in the spatial dimension and the range dimension preserves the identity of each pixel in the clean image, thereby giving the best output.

2. The PSNR value is more than 50 dB for all clean images in the database proving the effectiveness of the mode seeking approach used by the filter algorithm.

3. For images corrupted with Gaussian noise of 10% and 20% variance σ_s and σ_r with values greater than '1' maximize the PSNR value indicating that a certain amount of smoothing is necessary to handle noise.

4. The peak in the PSNR value becomes less pronounced with increase in the noise in the input image for the algorithm. Beyond 20% noise, there is no distinct peak showing that mean shift filtering does not help.

5. The best value of σ_s and σ_r are proportional to noise for noise amounts less than 20%.

3.10 Conclusions

The performance of the mean shift filter on images corrupted with Gaussian noise was studied. Our expectations based on a qualitative understanding of the filter were substantiated by the experimental results. These experiments have given useful inputs for understanding and optimizing the performance of the mean shift filter in the presence of noise. The conclusion is that the mean shift vector concept for detecting the modes in the image has the potential to identify the regions of interest in a noisy image when used with optimal values of σ_s and σ_r . Finally, mean shift filter handles noise robustly till the noise in the image is less than about 20%. To handle images with higher amount of noise, there is a need for better

algorithms. The next chapter discusses the research carried out on the variants of the mean shift filter for improving its performance.

Chapter 4

Study of the Mean Shift Filter on Noisy Images

4.1 Introduction

The previous chapter has explained the initial work carried out on understanding the behavior of the mean shift filter as a function of the normalization constants. Identifying values for σ_s and σ_r which give the best PSNR for the output image is not easy; also, their performance is limited to images with noise less than 20%. This chapter describes studies on developing variants of the Mean Shift filter to see if there is any improvement in output quality or decrease in dependence on σ_s and σ_r as inputs to the algorithm.

4.2 Variants of Mean Shift Filter

The experiments on the Mean Shift filtering technique and its performance on noisy images led to design of variants of this filter. Intuition gave the following inputs for the development of variants.

- Compared to the mean, the median is a robust statistic. Using the median shift vector instead of the mean shift vector should give a filter which is more tolerant to noise in the images.

- The mean shift filter gives equal weights to all the buckets in the neighborhood thus leading to an unbiased estimate in which the clean and noisy

pixels get the same weightage in the mode seeking process. If the buckets containing the noisy pixels are prevented from entering the neighborhood region of the candidate pixel for which the mean shift vector is being calculated, the filtered output so obtained will not contain the noisy pixels. Using a statistic like the variance to allow or deny a bucket to enter the mean shift vector neighborhood is an approach to give preference to certain buckets containing clean pixels as compared to buckets containing noisy pixels.

- Extending the concept mentioned earlier, it is possible to extract regions by specifying two values for the statistic like the variance. This ensures that buckets which have a value of the statistic in between the specified two values will enter the mode seeking process. This approach is useful in region extraction when a-priori estimate of lower and upper bounds of the statistic is available.

- In the process of mode seeking in the neighborhood, the mean shift filter considers equal sized buckets based on the value of σ_s and σ_r. Using a statistic like variance to identify buckets of unequal size is likely to detect both the weak and strong features in the presence of noise.

The above inputs based on intuition led to design of the following four variants of the mean shift filter.

1. Median shift filter
2. Weighted mean shift filter
3. Multi-threshold mean shift filter
4. Variable bucket size mean shift filter

4.3 Filter variants and Algorithms

Using the mean shift filter as the basic filter, we have designed the following variants. While the first of these filters uses the median of the pixels for calculating the mean shift vector, for the remaining three filters the variance of the pixels within a bucket plays an important role. We felt that the variance of the pixels within a bucket is indicative of the amount of noise and could be used to guide

the mean shift vector. The theory behind each filter is briefly explained and is followed by a description of the algorithm used for implementing each filter.

4.4 Median shift filter

Though the mean is computationally a better statistic it is less robust than the median. The median is less susceptible to outliers and is robust until the number of outliers reaches 50% of the total population. As mentioned earlier, the basic intuition is that while mean shift when applied to noisy images could lead to buckets not necessarily belonging to regions of interest (ROI), median shift would perform better because of the inherent robustness of the median.

Algorithm

If $x_{j=1\cdots n}$ and $z_{j=1\cdots n}$ be the d-dimensional original and filtered image points in the joint spatial-range domain. The superscripts **s** and **r** are used to indicate the spatial and range parts of the vectors, respectively. The original image data is normalized with the constants σ_s and σ_r for the spatial and the range part respectively.

For each $j = 1 \cdots n$

- **Step 1** : Initialize k = 1 and $y_k = x_j$.
- **Step 2** : Compute y_{k+1} = Median(all pixels x in the neighborhood of k) , k $\leftarrow$ k + 1 till convergence.
- **Step 3** : Assign $z_j = (x_j^s, y_{conv}^r)$

The filtered data at the spatial location of x_j will have the range components of the point of convergence y_{conv}.

4.5 Weighted mean shift filter

The mean shift filter while calculating the mean shift assigns equal weight to all the buckets in the 27-bucket neighborhood. We felt that this condition is not necessary for all images. Buckets, which lie in the regions of interest should get

preference over those which do not. To choose the buckets of interest, we used the variance of the pixels in the bucket as a deciding factor. Buckets, whose variance is less than a specified variance threshold T, were qualified to enter the mean shift filter. Those buckets whose variance was more than the threshold were disqualified. Binary weighting was used causing only some buckets to enter the filtering process although other "soft" weighting functions can also be used.

Algorithm

For each $j = 1 \cdots n$

- Step 1 : Initialize k = 1 and $y_k = x_j$.
- Step 2 : Compute $y_{k+1} = \frac{1}{n_k} \sum_{x_i \in S(y_k) and Variance[S(y_k)] < T)} x_i, k \leftarrow k + 1$ till convergence.
- Step 3 : Assign $z_j = (x_j^s, y_{conv}^r)$

4.6 Multi-threshold mean shift filter

Two thresholds T_1 and T_2 and a majority value M are given as input to this filter. While carrying out mean shift filtering, the filter selects a candidate bucket from the 27-bucket neighborhood for calculation of the mean shift vector, if the candidate bucket's variance is less than the threshold T_1. If the variance lies between T_1 and T_2 the filter will examine the 27 neighbors of the candidate bucket. If the number of neighbors having variance less than T_1 is M or more then the candidate bucket is accepted for mean shift filtering, otherwise it is rejected. If the variance of the candidate bucket is more than T_2, then the bucket is rejected outright. Obviously, the values of T_1, T_2 and M have a significant effect on the filtered output.

Algorithm

For each $j = 1 \cdots n$

- Step 1 : Initialize k = 1 and $y_k = x_j$
- Step 2 : Find the bucket of y_k , denoted by Bucket (y_k) .
- Step 3 : For Bucket (y_k) find the variances of all neighboring buckets denoted by the set V.

- Step 4 : For each element ,E in the set V,

  if ($value < T_1$) then accept the element.

  else if ($T_1 < value < T_2$)

  { repeat Step 2 for the element, E and find the set V_E. if (number of elements in set V_E with $variance < T_1$) < M then accept the element. Else reject the element. } else if ($value > T_2$) reject the element. [At this stage the set V contains all buckets which are acceptable]

- Step 5 : Compute $y_{k+1} = \frac{1}{n_k} \sum_{x_i \in V} x_i$, k ← k + 1 till convergence.

- Step 6 : Assign $z_j = (x_j^s, y_{conv}^r)$

4.7 Variable bucket size mean shift filter

Unlike the mean shift filter, which uses buckets of equal sizes, we have designed this filter to use buckets of variable and unequal sizes. The image, which is initially of size 256 x 256, is split into four equal sized quadrants. Each of these quadrants is recursively split if the variance is greater than a threshold T. As a result, areas of high variance, i.e noisy region, have smaller buckets than more uniform (less variance) regions. The regular mean shift filter is applied to the image with these unequal sized buckets.

Algorithm

- Step 1 : Split the input image using quadtree into 4 quadrants.

- Step 2 : For each quadrant calculate the variance.

- Step 3 : If the $variance < T$ then the quadrant is a leaf in the quadtree Else repeat Step 1 and Step 2 for each $j = 1 \cdots n$

- Step 4 : Initialize k = 1 and $y_k = x_j$.

- Step 5 : Compute $y_{k+1} = \frac{1}{n_k} \sum_{x_i \in S(y_k)} x_i$, k ← k + 1 till convergence.

- Step 6 : Assign $z_j = (x_j^s, y_{conv}^r)$

4.8 Experiments

The initial experiments were conducted using all the four algorithms on the cameraman, pepper and Lena images and their 10% and 20% noisy versions.

4.9 Results

The results of our initial experiments with the sample images using the median shift algorithm are shown in Figure 4.1 to Figure 4.3 for cameraman, peppers and Lena respectively. The quantitative results are shown in Table A.5 of the Chapter 7. Comparing the results in Table A.1 and Table A.5 indicate that for all the three sample images the PSNR value is reduced by 3 to 6 dB for the 10% noise case for the median shift filter compared to the mean Shift filter. Similarly there is an increase in the region count and decrease in the Pratt's figure of merit for the edge quality due to over-segmentation. This is qualitatively also confirmed by the outputs shown in Figure 4.1 to Figure 4.3. This is found true for the 20% noise case also. The results indicate that the mean shift filter output is better than that of the Median Shift filter. Hence the remaining images in the database were not tested with the median shift filter.

Similarly the results for the sample images with weighted mean shift filter are shown in Figure 4.4 to Figure 4.7. The values for PSNR, region count and Pratt's figure-of-merit are similar to that for the mean shift filter. One important parameter which is an input to this filter is the variance limit as mentioned in the description of algorithm in the earlier section. This parameter decides which of the buckets in the neighborhood of a pixel will be considered for the computation of the mean shift vector. It was found that for all the sample images the PSNR of the filtered image shows a peak when this parameter is set to a value less than the variance of the noise in the image. This behavior was observed for both 10% and 20% noise cases. The remaining images in the database were also tested with this filter and the behavior was confirmed. The quantitative results for all the images are shown in Table A.6 to Table A.8.

The results for the variable bucket size mean shift filter are shown in Figure 4.8 to Figure 4.11. The quantitative results indicate that the PSNR value and Pratt's figure-of-merit are same as that for the mean shift filter. But more regions are

detected by this filter. This is found to be true for a majority of the images in the database. A higher value of region count for almost the same value of PSNR means that there is an improvement in the output quality. Comparison of Figure 4.8 to Figure 4.11 with the corresponding images in Figure 3.3 to Figure 3.6 indicate the presence of more regions in the filter output. The quantitative results for all the images are shown in Table A.9 to Table A.11. An important observation for this filter is its better performance in detecting weak features in images. Such features are more seen in the boat image than the remaining images in the sample set. Comparison of Figure 4.8 and Figure 3.3 shows that in the case of the variable bucket size filter there are fewer cuts in the mast of the boat for the edge output. The multi-threshold mean shift filter (which is basically the weighted mean shift algorithm with two thresholds) did not show better performance than the weighted algorithm.

A few key observations are listed below.

1. Comparison of Table A.1 to Table A.4 and Table A.6 to Table A.8 indicates that the performance of the weighted mean shift filter is similar to the mean shift algorithm. The weighted algorithm did not outperform the mean shift algorithm because it could not eliminate any neighboring bucket on the basis of variance. Thus, in the absence of major difference in variance values between neighboring buckets, the weighted mean shift tends to behave like the regular mean shift algorithm.

2. Qualitatively, the comparison of the weighted algorithm's filtered, segmented and edge detected outputs are similar to that of the mean shift algorithm.

3. The weighted algorithm shows sensitivity to the variance threshold. For the 10% (standard deviation of noise) case, the variance threshold of 95(a value below 100) causes the filter output to give the maximum value of the PSNR. Similarly for the 20% case, the variance limit of 380(a value below 400) causes the filter output to give the maximum value of the PSNR. In the former case the variance of the noise is 100 and in the latter it is 400. When the variance limit is reduced from 95 to 50, the PSNR value is found to reduce. Similarly, it gets reduced as the variance limit is increased above 100. A similar behavior is observed with 20% noise contaminated image

also. This indicates the presence of a point of inflexion for the PSNR with respect to variance limit value of the algorithm. This reinforces our earlier hypothesis of the "peaking" behavior of the mean shift filter based on the size chosen for the spatial and the range buckets.

4. The comparison of data in Table A.9 to Table A.11 and Table A.1 to Table A.3 tells how the variable bucket size mean shift filter performs compared to the regular mean shift algorithm. An important observation is that while PSNR value is slightly lower for the former case compared to the latter, the region count which indicates the number of regions in the segmented output is better for the former.

5. Qualitatively, the results of the variable bucket size mean shift filter are better than the remaining two filters for all the three sample set images. This is indicated by the detection of the small features in the filter output. This can be observed by comparing the results in the corresponding images in Figure 4.4 to Figure 4.11. Quantitatively, for the same value of PSNR more number of regions are detected by this algorithm.

4.10 Conclusions

Some of the significant conclusions on the variant algorithms are listed below.

1. The median shift algorithm does not seem to be suitable for filtering of images contaminated with Gaussian noise.

2. The weighed mean shift filter does not appear to be suitable for images in which the noise is uniformly spread on the entire image. However, this seems to be a good candidate for images in which noise is localized to limited regions. More research on such types of images needs to be carried out. The multi-threshold mean shift filter which replaces the single threshold of the weighted algorithm with two thresholds has not shown any improvement compared to the latter case for the sample set.

3. The variable bucket size filter performs well qualitatively even for the highly noisy images (with 20% standard deviation of Gaussian noise). Quantita-

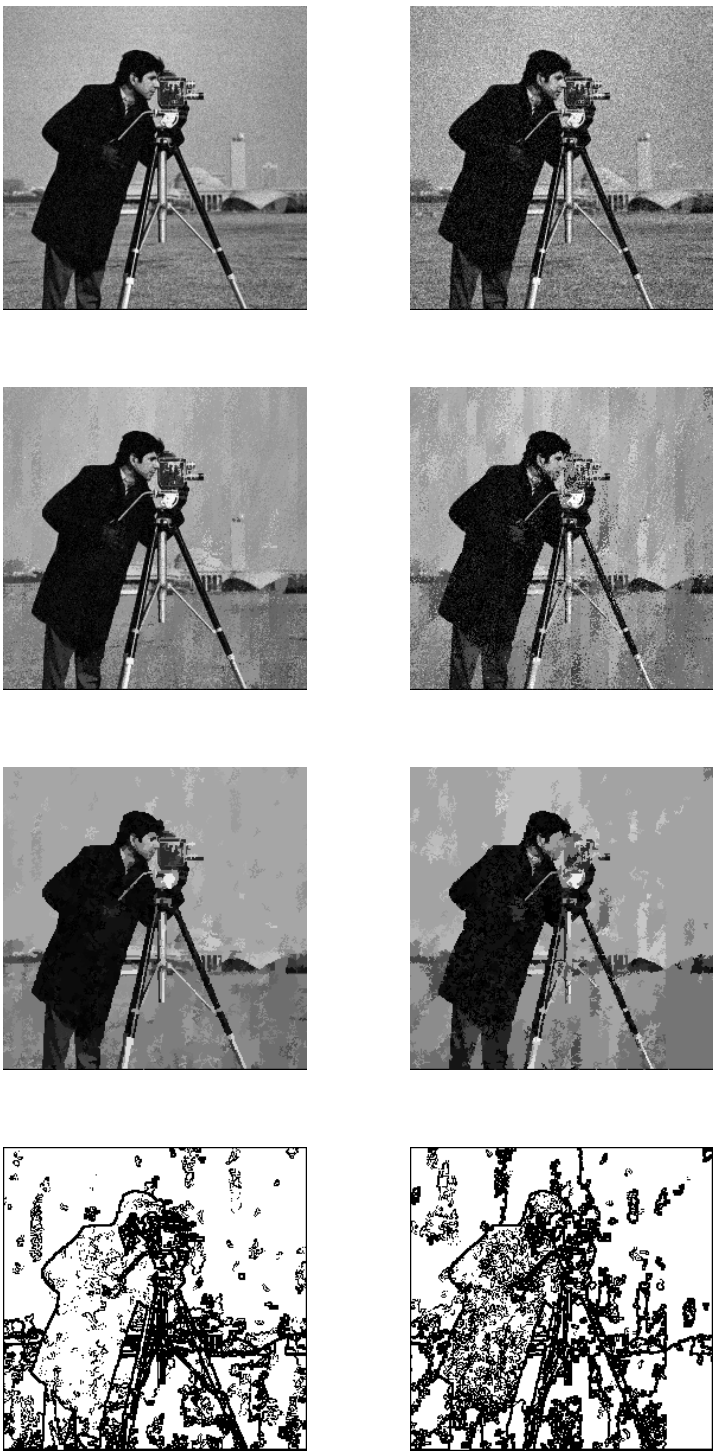

Figure 4.1: Comparative performance of median shift filter on cameraman image with 10% noise(first column) and 20% noise(second column). The filtered outputs are in the second row, the segmented outputs in the third row and the edges in the fourth row.

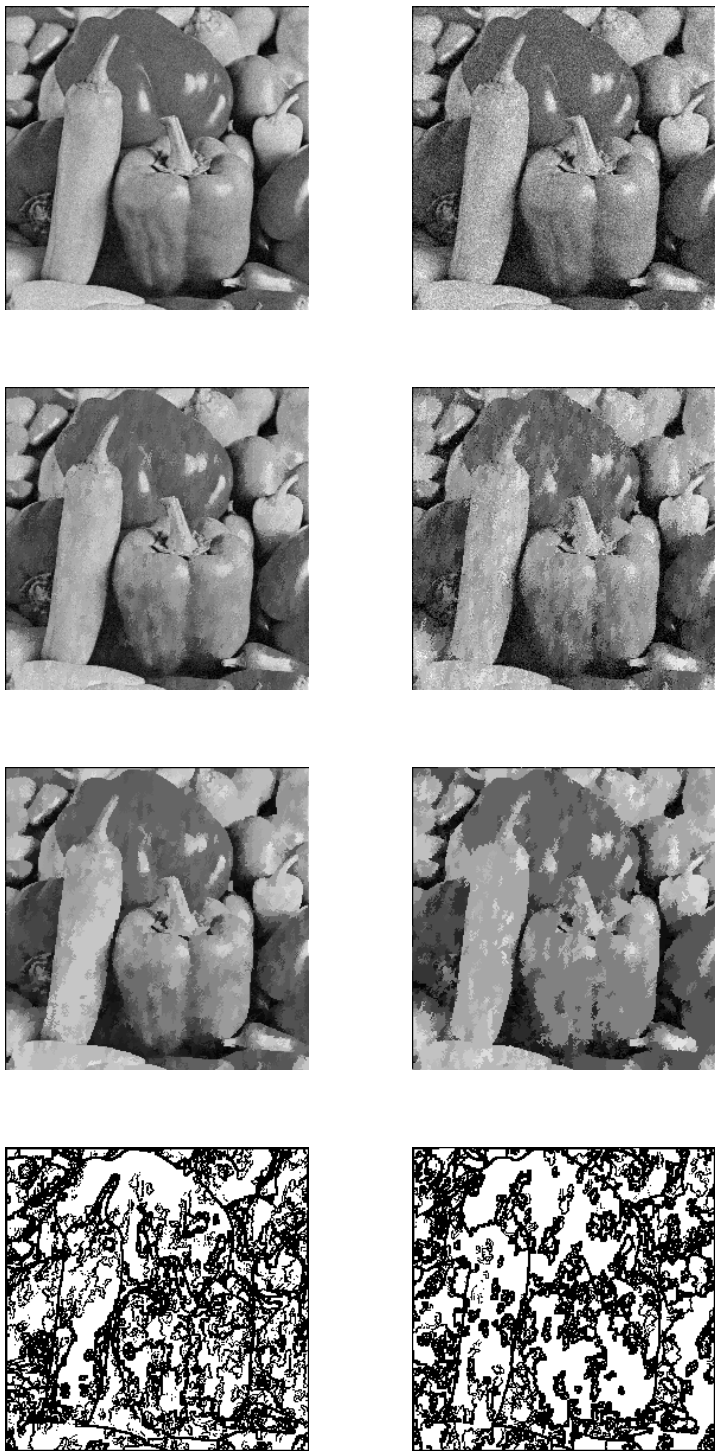

Figure 4.2: Comparative performance of median shift filter on peppers image with 10% noise(first column) and 20% noise(second column). The filtered outputs are in the second row, the segmented outputs in the third row and the edges in the fourth row.

Figure 4.3: Comparative performance of median shift filter on Lena image with 10% noise(first column) and 20% noise(second column). The filtered outputs are in the second row, the segmented outputs in the third row and the edges in the fourth row.

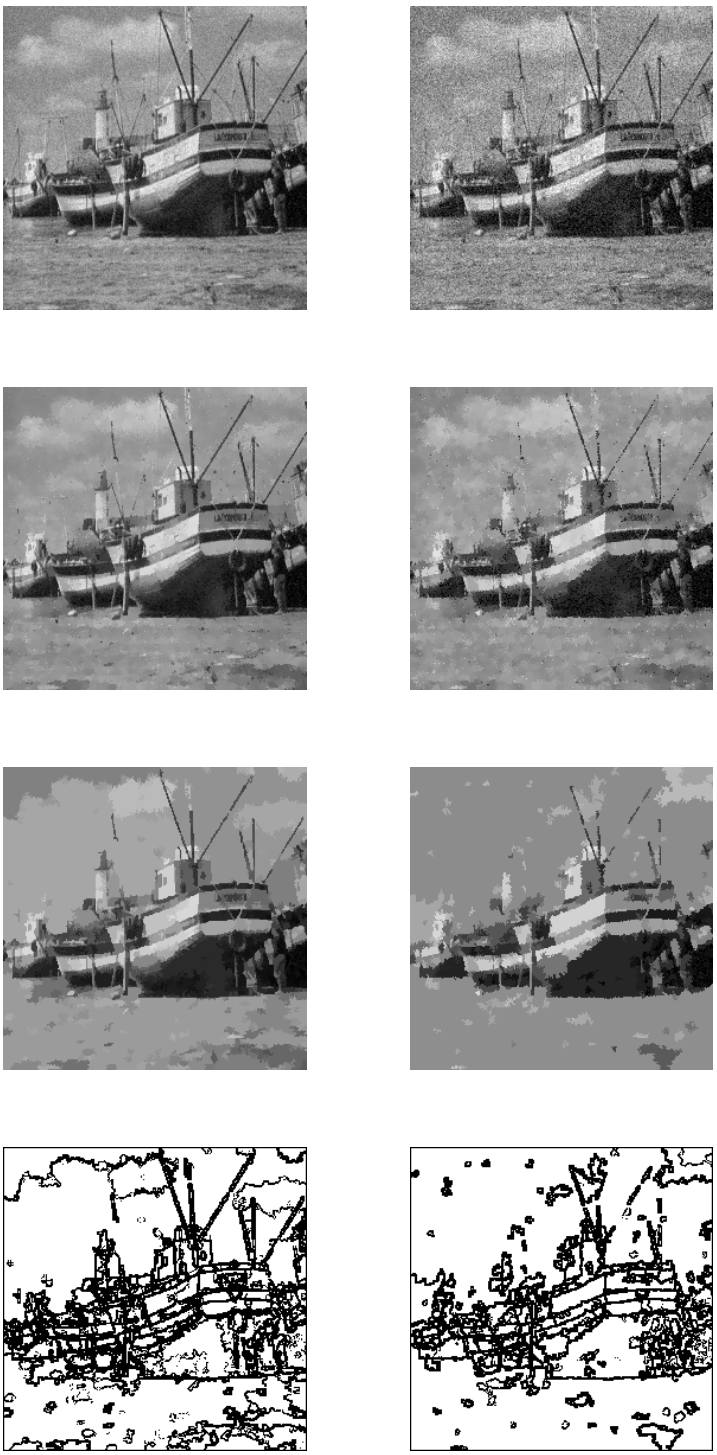

Figure 4.4: Comparative performance of weighted mean shift filter on boat image with 10% noise(first column) and 20% noise(second column). The filtered outputs are in the second row, the segmented outputs in the third row and the edges in the fourth row.

Figure 4.5: Comparative performance of weighted mean shift filter on cameraman image with 10% noise(first column) and 20% noise(second column). The filtered outputs are in the second row, the segmented outputs in the third row and the edges in the fourth row.

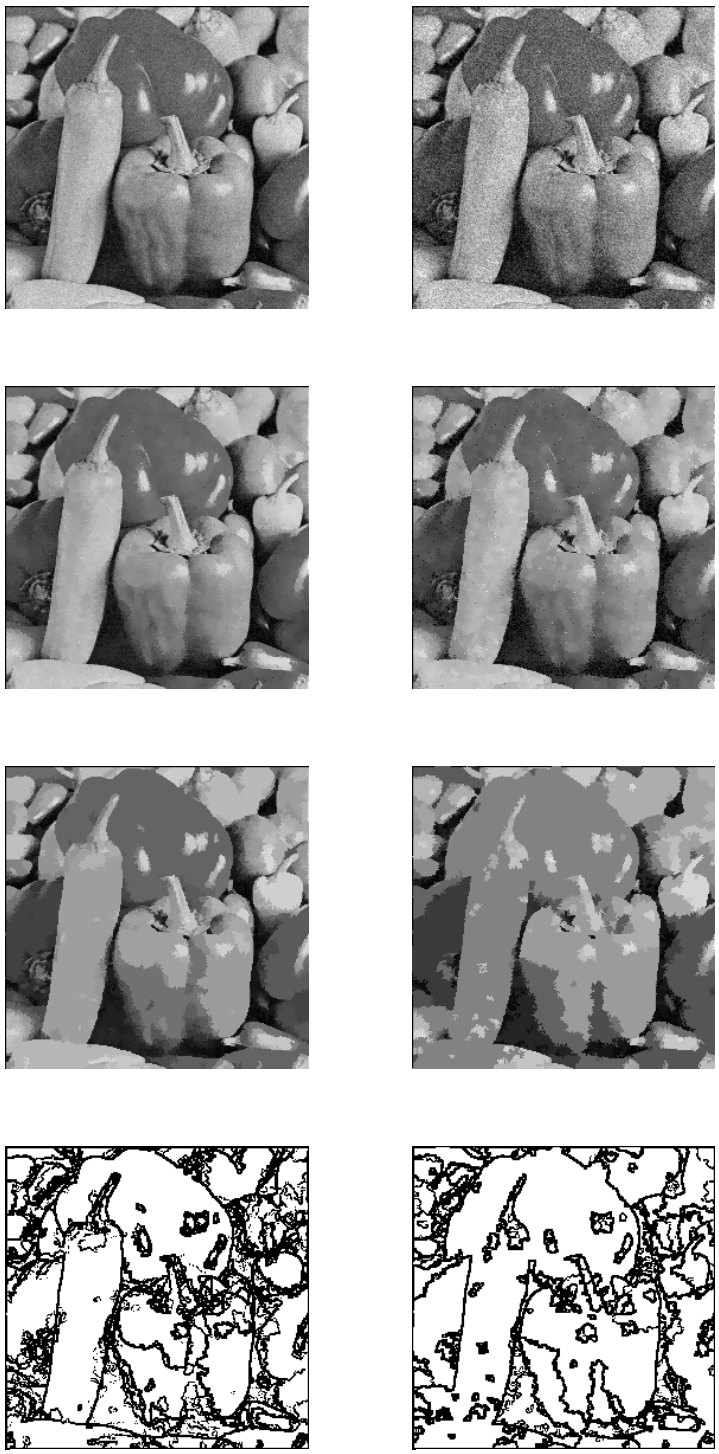

Figure 4.6: Comparative performance of weighted mean shift filter on peppers image with 10% noise(first column) and 20% noise(second column). The filtered outputs are in the second row, the segmented outputs in the third row and the edges in the fourth row.

Figure 4.7: Comparative performance of weighted mean shift filter on Lena image with 10% noise(first column) and 20% noise(second column). The filtered outputs are in the second row, the segmented outputs in the third row and the edges in the fourth row.

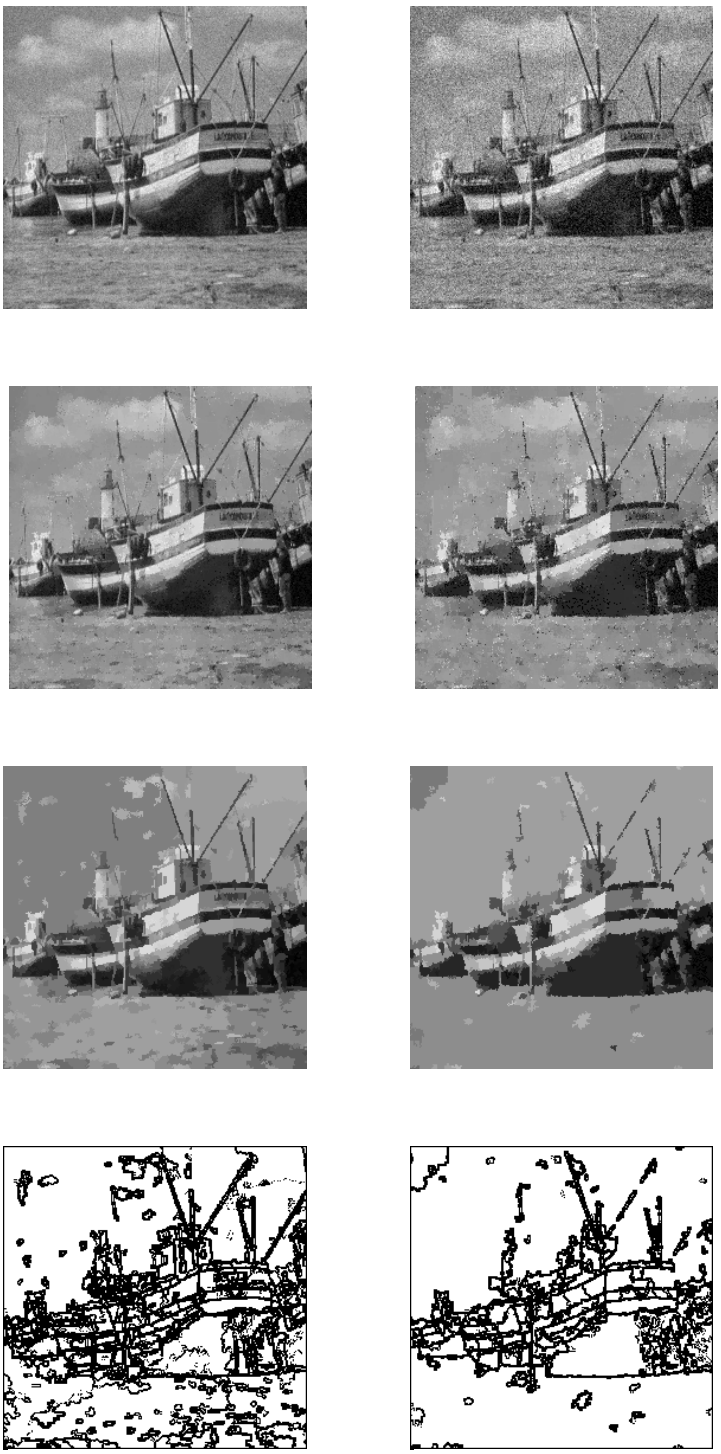

Figure 4.8: Comparative performance of variable bucket size mean shift filter on boat image with 10% noise(first column) and 20% noise(second column). The filtered outputs are in the second row, the segmented outputs in the third row and the edges in the fourth row.

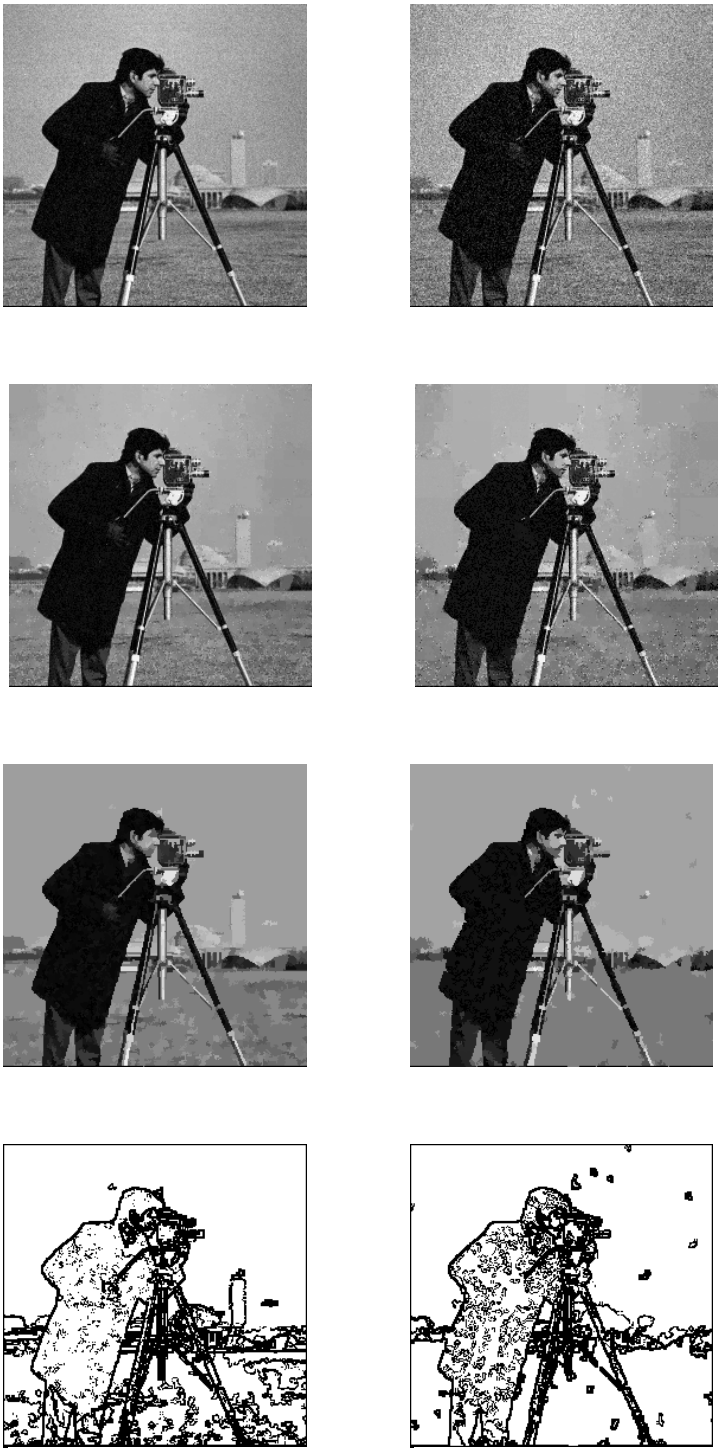

Figure 4.9: Comparative performance of variable bucket size mean shift filter on cameraman image with 10% noise(first column) and 20% noise(second column). The filtered outputs are in the second row, the segmented outputs in the third row and the edges in the fourth row.

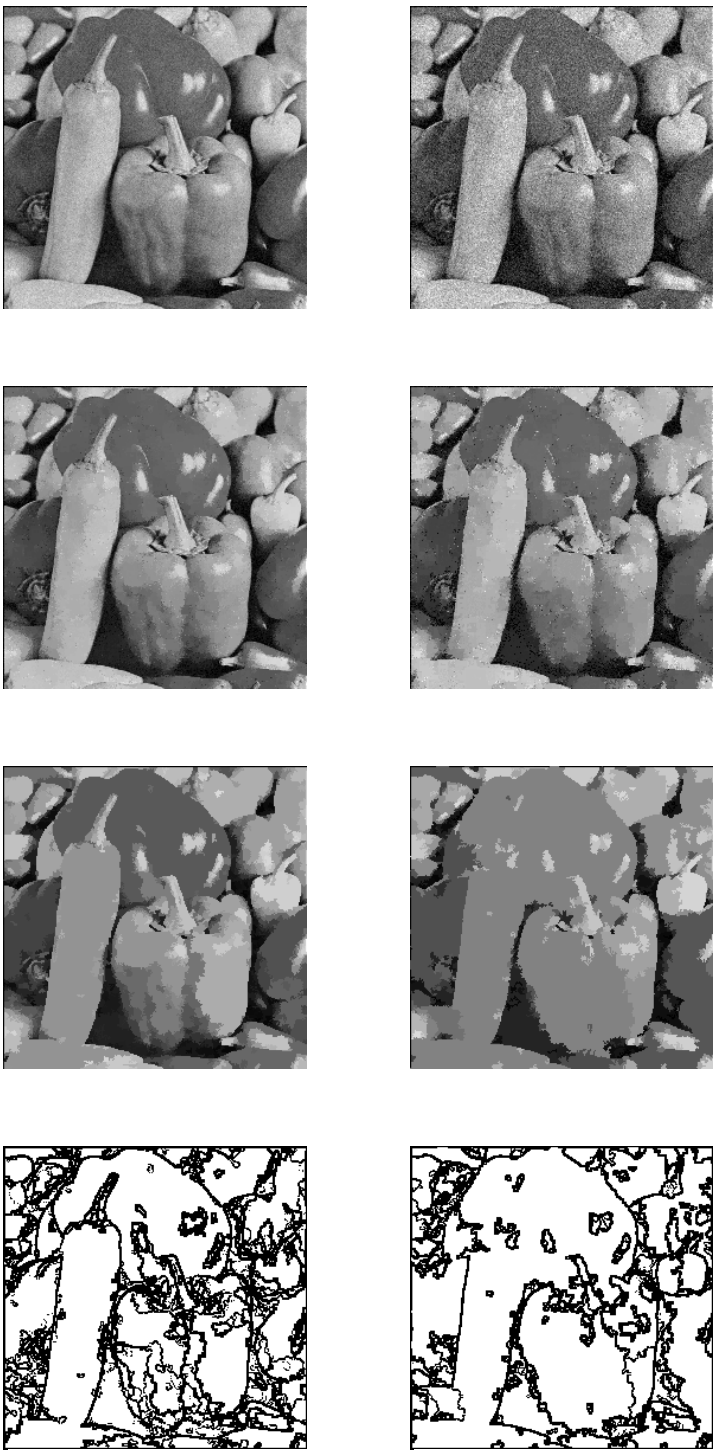

Figure 4.10: Comparative performance of variable bucket size mean shift filter on peppers image with 10% noise(first column) and 20% noise(second column). The filtered outputs are in the second row, the segmented outputs in the third row and the edges in the fourth row.

Figure 4.11: Comparative performance of variable bucket size mean shift filter on Lena image with 10% noise(first column) and 20% noise(second column). The filtered outputs are in the second row, the segmented outputs in the third row and the edges in the fourth row.

tively, the number of regions after segmentation are greater for this algorithm compared to the remaining two.

4. Thus the weighted mean shift filter and the variable bucket size filter are suitable for robust filtering of Gaussian noise contaminated images. Both these algorithms use the region properties to identify the modal pixels. While in this research variance was used as a decision criteria, it is possible to use other criteria which are more relevant for the feature space. Thus outlier rejection in non parametric estimation can consider these algorithms for achieving robustness.

5. The research on these variants of the Mean Shift filter indicates that it is possible to improve the performance of this filter and images having upto 20% Gaussian noise can be filtered without losing the small features. With higher amounts of noise in the input image, there is need for a different approach. This is discussed in the next chapter.

Chapter 5

Stochastic Resonance and Mean Shift Filter for Highly Noisy Images

5.1 Introduction

In Chapter 3 the research on the impact of choosing different values for the two constants and how they affect the output quality in the presence of noise was discussed. In Chapter 4 the variants developed for the mean shift filter were compared qualitatively and quantitatively. In continuation, a novel technique which combines stochastic resonance with mean shift filtering for handling images corrupted with large amounts of Gaussian noise i.e noise greater than 20% is discussed in this chapter.

5.2 Combining Stochastic resonance and Mean Shift filter

The basic aspects of stochastic resonance (SR) have been discussed in Chapter 2 in the literature survey. As mentioned earlier SR occurs when the signal-to-noise ratio of a nonlinear device is maximized for a moderate value of noise intensity. It often occurs in bistable and excitable systems with subthreshold inputs. For lower noise intensities, the signal does not cause the device to cross threshold, so little

signal is passed through it. For large noise intensities, the output is dominated by the noise, also leading to a low signal-to-noise ratio. For moderate intensities, the noise allows the signal to reach threshold, but the noise intensity is not so large as to swamp it. Thus, a plot of signal-to-noise ratio as a function of noise intensity shows an upside-down "U" shape.

We draw a parallel between the functioning of a mean-shift filter (in particular and kernel density estimation techniques in general) and double-well potential systems. The equilibrium state of the mean-shift filter is defined by a set of modes which characterize the potential wells. The pixels in the original image (given by their distribution in the $3D$ or $5D$ feature spaces) take their filtered values (modes), i.e. settle down in a potential well following a path defined by the successive mean shift vectors.

The potential barrier is a function of the difference in the mean shift vectors that lead to the different mode values. For example, if two mode values differ only slightly in the paths taken by pixels, then even a small amount of noise causes a pixel to move from one mode to another. In other words, the potential barrier between two such modes is small. The potential barriers are correspondingly large if the paths leading to the mode values are significantly different. As the computation and updates of the mean shift vector are critically dependent on the distributions of pixels within a bucket and its neighboring buckets, the potential barriers are equally dependent on the bucket structure. As a specific case of the bucket structure, the potential barrier between two mode values is high if the buckets are small in size. A small bucket defines a similarly small neighborhood and restricts the number of pixels that participate in the calculation of mean shift vectors. Consider two pixels separated by a distance d in the 3D feature space. If the bucket sizes are small in comparison to d, the two pixels fall in different neighborhoods, influence each other less and are more likely to reach different mode values. That is, the potential barrier is high. On the other hand, if the bucket size is large in comparison to d, the two pixels are likely to be in the same neighborhood and have a greater likelihood of having similar mean shift vectors and reaching the same mode value. Therefore, in this case, the potential barrier may be characterized by the bucket size: the smaller the bucket size, the larger the potential barriers and vice versa.

The output from mean shift filter is a set of modes and their associated local neighborhoods. Each such neighborhood is commonly taken to define a segment and one of the successful applications of mean shift filter has been in image segmentation [83] and edge detection. We find that image segmentation may be compared with the potential well problem as follows. The mode is the representative of the segment. A pixel in the middle of the segment has a well defined path to its mode because of the averaging process of the mean shift filtering algorithm due to which the effect of any disturbance like noise is reduced. On the other hand, for a pixel at the boundary between two regions could have a path to the modes associated with any of the two regions. This situation is analogous to the double-well problem in which electric charges can move towards any one of the two wells. The wells are analogous to the regions, the electric charges are analogous the pixels and the potential barriers are analogous to the difference in the two mode values as a function of the bucket size. The segmented output is analogous to the distribution of the charged particles into multiple potential wells each corresponding to a different segment. So the bucket sizes are related to the noise characteristics and the sizes that resonate with the underlying pixel distributions may be expected to provide a higher performance.

Our first attempt at combining SR with mean-shift filtering is in the empirical spirit and is relatively naive. This approach led to the development of a Stochastic Bucket algorithm. A more rigorous approach is described in Section 5.8 and 5.9 after fully presenting the experiments and results of the stochastic bucket algorithm.

5.3 Stochastic Bucket Algorithm

From the relationship between potential double well problem and mean shift filtered output we felt that Stochastic Resonance may help us circumvent the problem of identifying the optimal values for normalization constants - σ_s and σ_r. Choice of σ_s determines which pixels fall into which well. There are two competing forces here: bias when small buckets are present, and mixture of different distributions when the bucket sizes are too large. Introducing noise into the size of the buckets allows stochastic resonance to produce correct filtered output when the underlying distributions resonate at the correct bucket size.

In this algorithm which we call the *Stochastic Bucket Algorithm*, we use the mean shift filter to generate multiple filtered outputs by choosing random values for σ_s and σ_r. These outputs are again thresholded and combined. By choosing different values for σ_s and σ_r, the algorithm chooses different bucket sizes thus causing the potential barriers between the modes to vary. This has the effect of varying the underlying potential well structure. It is expected that some of the potential well structures resonate with the image segments leading to better pixel distributions.

Steps of the Algorithm

- Step 1 : Input the minimum and maximum values for σ_s and σ_r for the mean shift filter.
- Step 2 : Input the number of outputs to be generated (N).
- Step 3 : Mean shift filter generates N filtered outputs by

  randomly selecting the values for σ_s and σ_r each time between the specified lower and upper bounds.
- Step 4 : Post-processing of the multiple outputs by

  (i) Generating a binary image for each filtered image using the mean value of the image as the threshold value.

  (ii) Obtaining the mean value of all the binary images.

The above algorithm was tested on a number of images and the results are described in the next section.

5.4 Experiments and results on noisy images with Stochastic Bucket Algorithm

The stochastic bucket algorithm was tested with the test database described in Chapter 3. Fixing the lower and upper bounds for σ_s and σ_r was a pre-requisite for using the algorithm. The following approach was followed for testing the algorithm with the noisy images.

1. The experiments are conducted using $2 \leq \sigma_s, \sigma_r \leq 8$ and $N = 25$. These values are chosen empirically from initial experiments where they are varied from 2 to 32 and N is varied from 10 to 40.

2. The stochastic bucket algorithm was run on the 120 images in the database. Performance is measured both qualitatively and quantitatively. For each image the PSNR, the region count and the edge figure-of-merit were calculated for quantitative evaluation. The filtered image, segmented image and edge image (using Sobel edge detector) were studied for qualitative evaluation.

Figure 5.1 shows the outputs obtained using the algorithm on the cameraman image. The first row shows the contaminated images with 10%, 20% and 30% Gaussian noise. The second row shows the filtered output.The third row shows the segmented output and the fourth row shows the edge detected output. The important observation is that even in the presence of 30% Gaussian noise, the stochastic bucket algorithm has been able to detect a weak feature like the tower in the background.

Figure 5.2 and Figure 5.3 show the results for the peppers and Lena images respectively. It was found that the quality of the results from stochastic bucket algorithm is highly variable. For example, the tower is not detected in the images with 10% and 20% noise whereas it is detected in other runs of the algorithm. This is attributed to the empirical nature of the algorithm and is addressed in the rigorous approach described in the next section. Hence it is recommended to repeat the algorithm on a noisy image to extract the weak features which may appear in some outputs and disappear in others.

5.5 Experiments on low contrast images with Stochastic Bucket Algorithm

The performance of the stochastic bucket algorithm was also evaluated on low contrast images.The test image was an extremely low contrast image of a car taken in the night using a digital camera. The image was tested with this algorithm. The result obtained was compared with the output obtained from mean shift filter algorithm alone. Figure 5.4 shows the outputs for this experiment.The observation

Figure 5.1: Application of stochastic bucket algorithm on cameraman image. First row shows the image with 10%,20% and 30% Gaussian.Second,third and fourth rows show the filtered,segmented and edge detected output images respectively for each of the noisy images. Note the detection of the tower in the 30% noise case.

Figure 5.2: Application of stochastic bucket algorithm on peppers image. First row shows the image with 10%, 20% and 30% Gaussian.Second, third and fourth rows show the filtered, segmented and edge detected output images respectively for each of the noisy images.

Figure 5.3: Application of stochastic bucket algorithm on Lena image. First row shows the image with 10%, 20% and 30% Gaussian. Second, third and fourth rows show the filtered, segmented and edge detected output images respectively for each of the noisy images.

from the experiment is that stochastic bucket algorithm outperforms the mean shift filter in the filtered output and the edge detected output. The input image is an extremely low contrast image and the car in the image is not visible to the human eye. After filtering with the mean shift filter, the output does not indicate again any features when seen by the human eye. However edge detection using a small value of the threshold parameter in the Sobel edge detector indicates in the edge output of the mean shift filter. Compared to this, the third row in Figure 5.4 which gives the results for the stochastic bucket algorithm shows the structure of the car in the filtered output. Similarly the edge output shows a better boundary for the car compared to that obtained from the mean shift filter. The stochastic bucket algorithm which applies SR to the mean shift filter output, boosts the weak signal of the car and makes it noticeable in the filtered image.

5.6 Experiments on very high noise images with Stochastic Bucket Algorithm

The stochastic bucket algorithm was also tested with the cameraman image with 50% Gaussian noise. The results obtained were again compared with the results obtained from the mean shift filter alone. The results are shown in Figure 5.5. In this figure, the results obtained by using the mean shift filter alone and by using stochastic bucket algorithm are compared. Qualitatively, even at 50% Gaussian noise in the input image, the stochastic bucket algorithm shows segments of the cameraman's coat though the remain segments are not very clear. In contrast, the mean shift filter output is the same as the input noisy image. In the edge detected images too, the stochastic bucket algorithm produces edges which are more continuous than those produced by the mean shift filter.

5.7 Study of Edge Models and Simulation

In order to further strengthen the practical results obtained with the stochastic bucket algorithm, research was carried out on edge models both theoretically and empirically. Subsequently, the algorithm was applied on noisy images for detecting weak features. This work has given the requisite foundation for proving that the

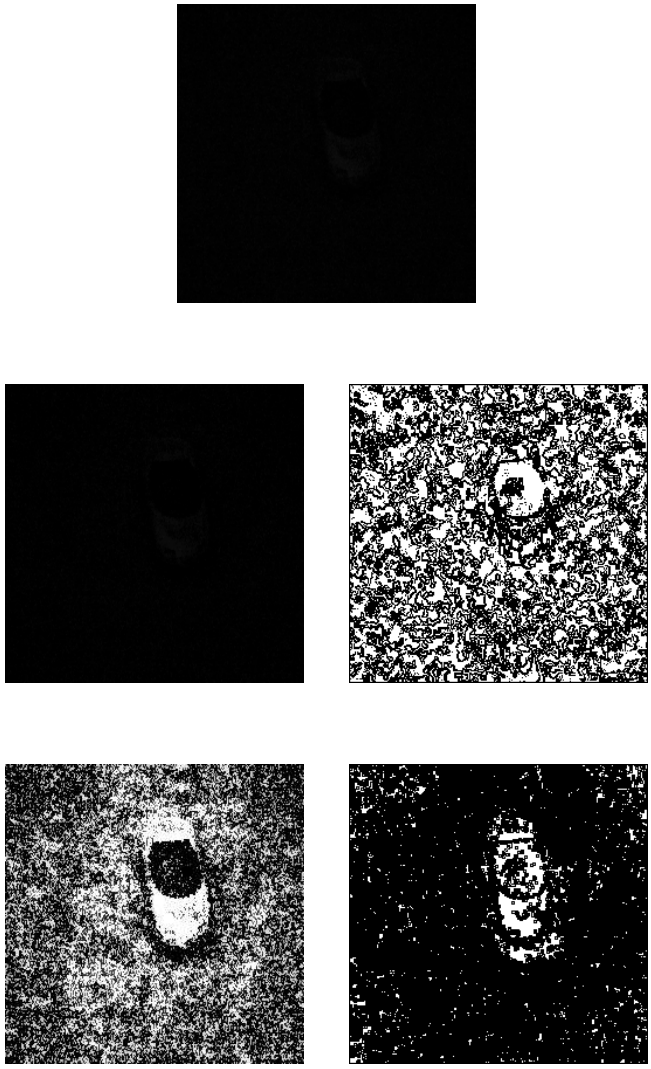

Figure 5.4: Comparative performance of mean shift filter and stochastic bucket Algorithm on a very low contrast image(top-most image). The second row indicates the filter and edge output for the mean shift filter. The last row indicates the same for the stochastic bucket algorithm.

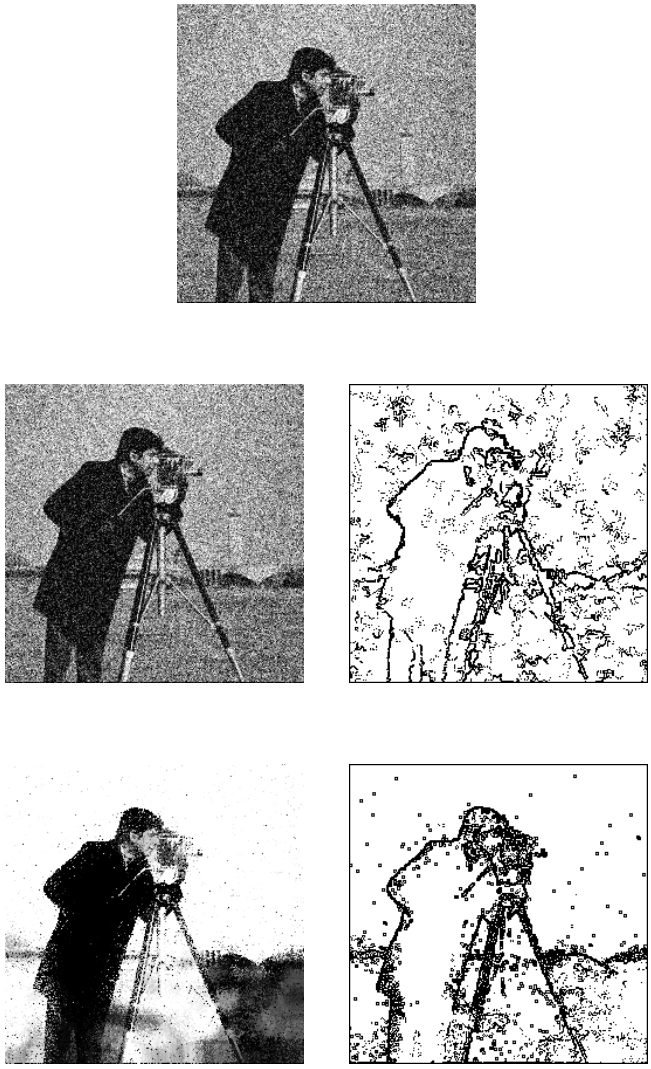

Figure 5.5: Comparative performance of mean shift filter and stochastic bucket algorithm on cameraman with 50% Gaussian noise(top-most image). The second row indicates the filter and edge output for the mean shift filter. The last row indicates the same for the stochastic bucket algorithm.

phenomenon of stochastic resonance exists in images with weak edges and can be used effectively for extracting weak features. The work proves the efficacy of stochastic resonance in boosting weak signals which is complementary to tolerance to noise exhibited by the mean shift filter. This work is explained in detail in the following sections.

5.8 Application of AMASE for SR

Consider a signal that lies entirely below a detection threshold and therefore is completely undetected. Adding moderate amounts of noise to such a signal causes the combination of signal and noise to cross the detection threshold without too much distortion of the characteristics of the original signal. With greater amounts of noise, the output becomes entirely dominated by noise characteristics and the signal is again undetectable. Therefore, SNR is low for both no noise and addition of large amounts of noise. SNR initially decreases until noise begins to dominate the signal. Thus, a plot of SNR versus added noise intensities shows an upside-down 'U' shape. The presence of such a curve is often taken as the evidence for SR in a system.

Several interesting systems that exhibit SR have been studied by Greenwood et. al in [87]. We follow the analysis presented there to show the existence of SR in image domain where weak signals are equated with narrow regions and low-contrast edges.

Consider a signal $s(t)$ and a detectability threshold a. The signal is detected if at any t_i, $s(t_i) \geq a$. Using a kernel k for estimating s, the minimum value of *asymptotic mean average square error* (AMASE) is shown in [87] to be

$$AMASE = \frac{5}{4} n^{-\frac{4}{5}} \left(\mu_2(K)^2 \frac{1}{n} \sum_{i=1}^{n} \frac{p(t_i)^2}{f(F^{-1}(p(t_i)))^2} \right)^{\frac{1}{5}} \left(R(K) \frac{1}{n} \sum_{i=1}^{n} \frac{p(t_i)(1-p(t_i))}{f(F^{-1}(p(t_i)))^2} \right)^{\frac{4}{5}} \tag{5.1}$$

where n is the number of samples, $\mu_2(k), R(K)$ are kernel constants and $p(t)$ is the kernel estimator. AMASE is the theoretical measure of the mean squared error commonly used as a goodness-of-fit estimate in model fitting. The general approach is to take a Taylor approximation of the least squared error [88]. A number of kernels — triangular, bi-weight, tri-weight, Epanechnikov — are popular in the vision community and we use the Epanechnikov kernel in this paper. The

Epanechnikov kernel [4] is given by $K(u) = (3/4)(1-u^2), |u| \leq 1$ and is radially symmetric. If we assume Normal error distribution and the Epanechnikov kernel, AMASE has been shown as

$$AMASE = \frac{5}{4} n^{-\frac{4}{5}} \left(\frac{1}{25n} \sum_{i=1}^{n} \left(\frac{a - s(t_i)}{\sigma^2} s'(t_i)^2 + s''(t_i) \right)^2 \right)^{\frac{1}{5}} \left(\frac{3}{5n} \sum_{i=1}^{n} \frac{\sigma^2 \phi\left(\frac{s(t_i)-a}{\sigma}\right) \phi\left(\frac{a-s(t_i)}{\sigma}\right)}{\psi\left(\frac{s(t_i)-a}{\sigma}\right)^2} \right)^{\frac{4}{5}} \quad (5.2)$$

In Equation 5.2, $\mu_2(k) = 1/5$ and $R(K) = 3/5$ and σ^2 is the noise variance that results in SR. s' and s'' are the first and second derivatives of s. We model the weak edges and narrow regions as step edges smoothed by a Gaussian and a narrow pulse respectively.

5.9 Simulation Studies

In this section, we show through simulation that weak edges when modeled by a smoothed step edge exhibit SR. A weak edge is modeled by an ideal step edge that is smoothed by a Gaussian filter and we write it as

$$s(x) = A \frac{1}{\sqrt{2\pi}\sigma} \int e^{-\frac{(x-\mu)^2}{2\sigma^2}} dx \quad (5.3)$$

where A is the edge magnitude and μ is the location of the edge. σ is the parameter used to represent the distortion in the ideal step edge caused by the imaging system. This approach is along the lines of that followed by John Canny[89]. The first and second derivatives are given by Equations 5.4 and 5.5.

$$s'(x) = A \frac{1}{\sqrt{2\pi}\sigma} e^{-\frac{(x-\mu)^2}{2\sigma^2}} \quad (5.4)$$

$$s''(x) = A \frac{\mu - x}{\sqrt{2\pi}\sigma^3} s'(x) \quad (5.5)$$

It is important to note that there are two σs now: the first is the σ present in Equation 5.2 and characterizes the added noise for SR; and, the second is the σ of the signal and its derivatives (Equations 5.3 to 5.5). This second σ that describes the signal is not present explicitly in Equation 5.2 and is really because of the weak-edge model of Equation 5.3.

Consider a signal given by Equation 5.3 with $A = 1.0, \mu = 0$ and $\sigma = 1.0$. The detectability threshold $a = 1.05$ which is slightly above the maximum value

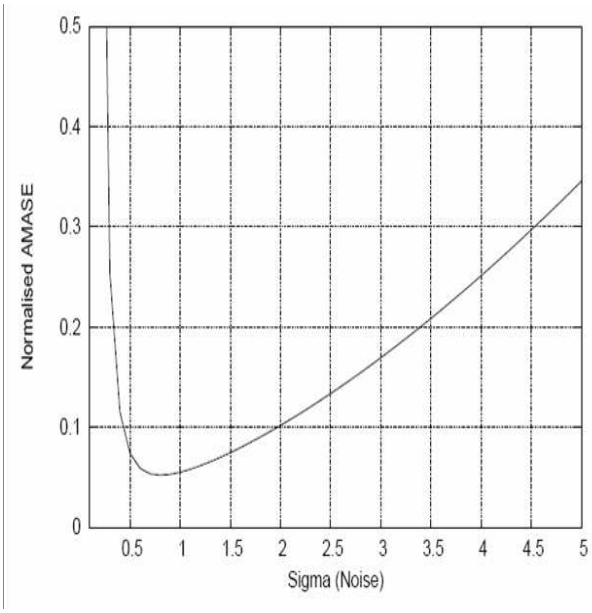

Figure 5.6: Theoretically calculated AMASE as a function of noise sigma (Equation 5.3)

of the signal making the signal undetectable. A plot of AMASE (Equation 5.2) for various values of added noise with σ ranging from 0.1 to 1.6 is shown in Figure 5.6. The AMASE values are normalized to the range $0-1$. The plot shows the characteristic minimum in AMASE value at $\sigma = 0.6$ indicating the occurrence of SR.

The theoretical analysis is confirmed by an empirical study. The weak step edge signal is given by the same equation (Equation 5.3). The threshold is set to the same value of $t = 1.05$. Note that the signal is *perfectly* estimated if the strength of the combined signal does not exceed the threshold for all samples that are to the left of the step edge and exceeds the threshold for all samples to the right of the step edge. We, therefore, measure the error as the number of samples that are detected above the threshold and are to the left of the edge location plus the number of samples that lie below the threshold to the right of the edge location. Initially, the error is 50% because the step edge does not exceed the threshold at all and there are as many samples to the left of the edge position (and therefore are correctly not detected) as there are to the right of the edge location (which are incorrectly not detected). Then, Gaussian noise with σ ranging from 0.1 to 1.6 is added to the signal.

Figure 5.7 to Figure 5.10 illustrate the empirical study. The step edge corre-

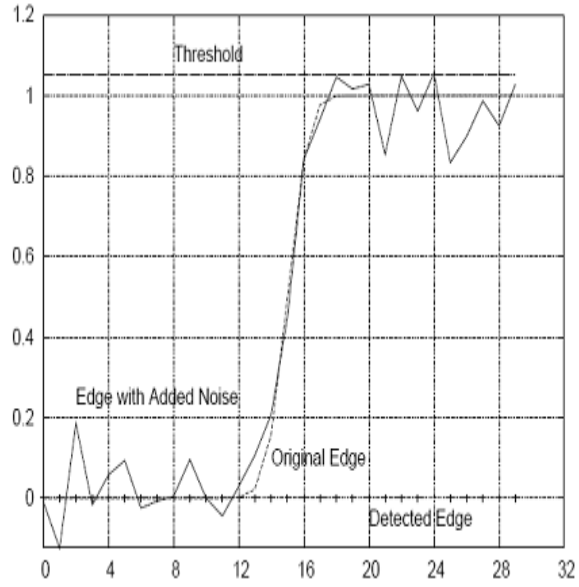

Figure 5.7: Weak edge corrupted with different amounts of noise ($\sigma = 0.1$)

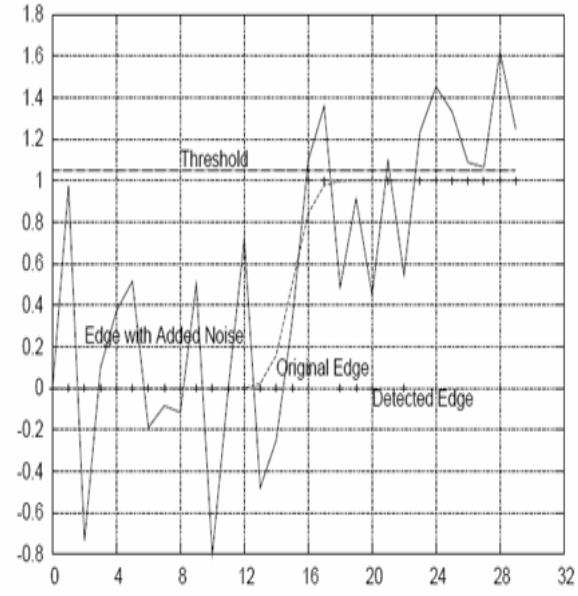

Figure 5.8: Weak edge corrupted with different amounts of noise ($\sigma = 0.4$)

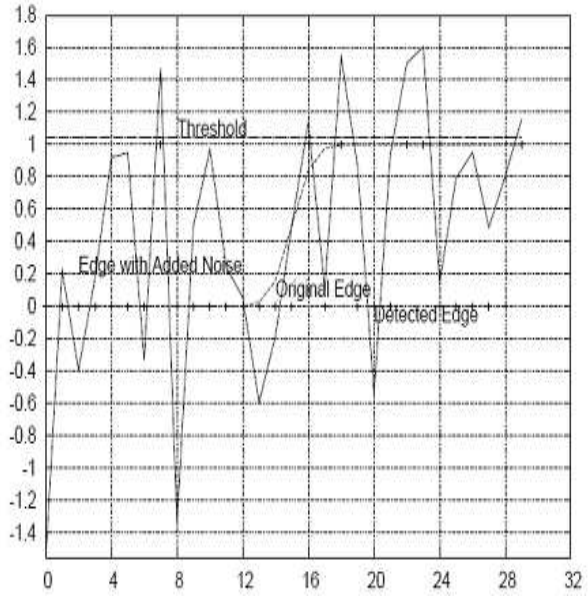

Figure 5.9: Weak edge corrupted with different amounts of noise ($\sigma = 0.75$)

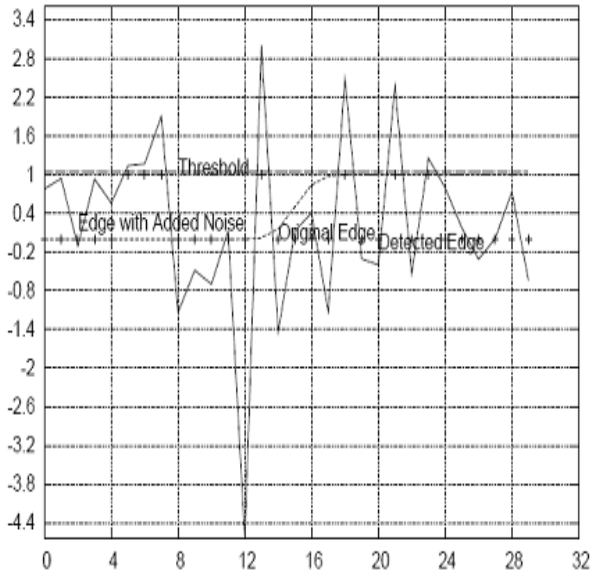

Figure 5.10: Weak edge corrupted with different amounts of noise ($\sigma = 1.5$)

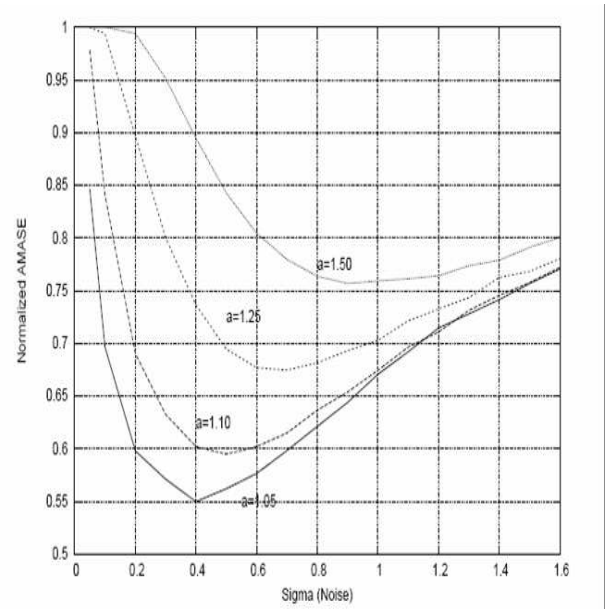

Figure 5.11: AMASE values calculated for images corrupted with different values of noise σ

sponding to Equation 5.3 is labeled *Original Edge* in the plots. *Edge with Added Noise* indicates the combined signal while the threshold value is shown as the horizontal line labeled *threshold*. If the value of the signal exceeds the threshold, then it is detected as a 1, otherwise it is undetected and has a value 0. *Detected Edge*, indicated by the '+' symbols, is the result of thresholding. It may be seen in Figure 5.7, with the addition of noise having $\sigma = 0.1$, only one sample (No. 24) is detected, i.e., exceeds or equals the threshold. Thus, the error is 46.67% (14/30), that is 14 out of the 30 samples are incorrectly estimated. Note that this is a small improvement over the initial error of 50%. As we increase the added noise to $\sigma = 0.4$, many more samples to the right of the step edge cross the threshold and are detected as seen in Figure 5.8. As we further increase the noise to $\sigma = 1.5$, many samples both to the left and right of the edge location cross the threshold and the error, consequently, increases. If the theory is correct and SR occurs, then there is a specific level of noise for which the error is minimized. A plot Figure 5.11 of the error versus σ (noise) confirms SR and shows the same characteristic as that of the theoretical AMASE curve of Figure 5.6. The minimum, however, appears at $\sigma = 0.45$ which is slightly lower than the theoretical value of $\sigma = 0.6$ which may be due to the discrete nature of the sampling in the empirical study. Note that the number of samples is set to 30 for the plots so that the analysis is clear.

In the calculations shown in Figure 5.11, the number of samples is 10000 and the experiment is repeated 20 times for each case to get more accurate estimates of the average errors. Other plots in Figure 5.11 are for different values of the detectability threshold a. As the value of a increases it indirectly makes the edges weaker and harder to detect. However, SR occurs in all the cases but we need to add *greater* amounts of noise, indicated by the increased values of σ (SR noise) at which the minima occur, to boost the increasingly weak edge strengths. The minima are also at higher values of AMASE which suggests that the improvement reduces with increasingly weak edge strengths (higher values of a). Also, the valleys are becoming shallower and it suggests that when the edges are extremely weak, SR may not help. In fact, when the threshold $a = 10$, it has been observed that there is no SR in that the AMASE curve does not show any minimum.

Similar theoretical and empirical analysis has been done for narrow regions which are modeled as a pulse of width $2a$ and height h. The smoothing is modeled as two different step edges — one going from low to high, and the other, from high to low — separated by $2a$. The results for such a case also show that SR occurs.

5.10 Experiments on noisy images with weak features

In this section, we show that mean-shift filter can be combined with SR to reveal weak edges and other features that are missed by applying mean-shift filter alone.

The outputs from mean-shift algorithm for three images corrupted by the addition of Gaussian noise of 10%, 20% and 30% are shown in Figure 5.12. For relatively low noise levels of 10% and 20%, mean-shift filter preserves weak edges and narrow regions. In Figure 5.12, in the left image in the second row, the two sets of three narrow masts each on top of the boat are clearly seen. There are also low-contrast edges on the tower to which the masts are fixed. These are also clearly seen. In center image in the second row, with noise of 20%, the masts are 'broken' and unclear, while in the right image in the second row, the masts are no longer visible and even the tower to which they are attached is so highly distorted in shape that it is virtually unrecognizable. These results support our hypothesis that robust techniques render undetectable certain features that are detectable in

the original images.

We applied SR to the mean-shift filtered output shown in the second row of Figures 5.12. As we know the parameters of the buckets used in the mean-shift algorithm, we know the size of the neighborhoods that participated in deriving the mean-shift. We used $\sigma_s = 4$ and $\sigma_r = 8$ for the highly noisy images and from the size of the buckets, we estimated the optimal noise sigma as $\sigma = 1.2$. It is done by using experiments similar to the ones described in Section 5.9 with varying values of σ for smoothing the step edges. These σ are analogous to the size of the buckets. We then added the optimal amount of noise to the mean-shift filtered output and thresholded each pixel using a local threshold. The local threshold is the average gray scale value in the neighborhood of the pixel. The final images so generated for the images in the second row of Figures 5.12 are shown in the last row of Figures 5.12.

It may be seen from the left image in the last row of Figure 5.12, that at low-noise levels, SR results in a cleaner image but appears to remove some low-contrast edges. Note the differences in the appearance of the tower on the boat. However, the narrow regions are preserved, if not improved. For higher noise levels, center and right images in the last row of Figure 5.12, it may be seen that the outputs continue to preserve and in the case of the right image in the last row Figure 5.12, even re-detect the narrow masts which were undetected in the original mean-shift output. The tower, which has become distorted in the right image in the second row corresponding to the Mean Shift filter, is also better detected. Thus, the addition of SR to mean-shift filter combines the tolerance to noise for gross features that mean-shift filter has with the ability to detect weak and narrow regions that SR gives. The result is noisy and there is a need to perform post-processing to clean up the image. We have done experiments directly on the 30% noise corrupted input image, but the image, as expected, is noisier than the one obtained when using mean-shift.

We tested the combination of SR and mean-shift filtering on a set of 40 images corrupted by 10%, 20% and 30% Gaussian noise (giving a set of 120 images) and found that the combination improves the performance of either if applied individually. In all these cases, the improvement is in the detection of the weak and narrow regions which were missed by the mean shift algorithm. The result

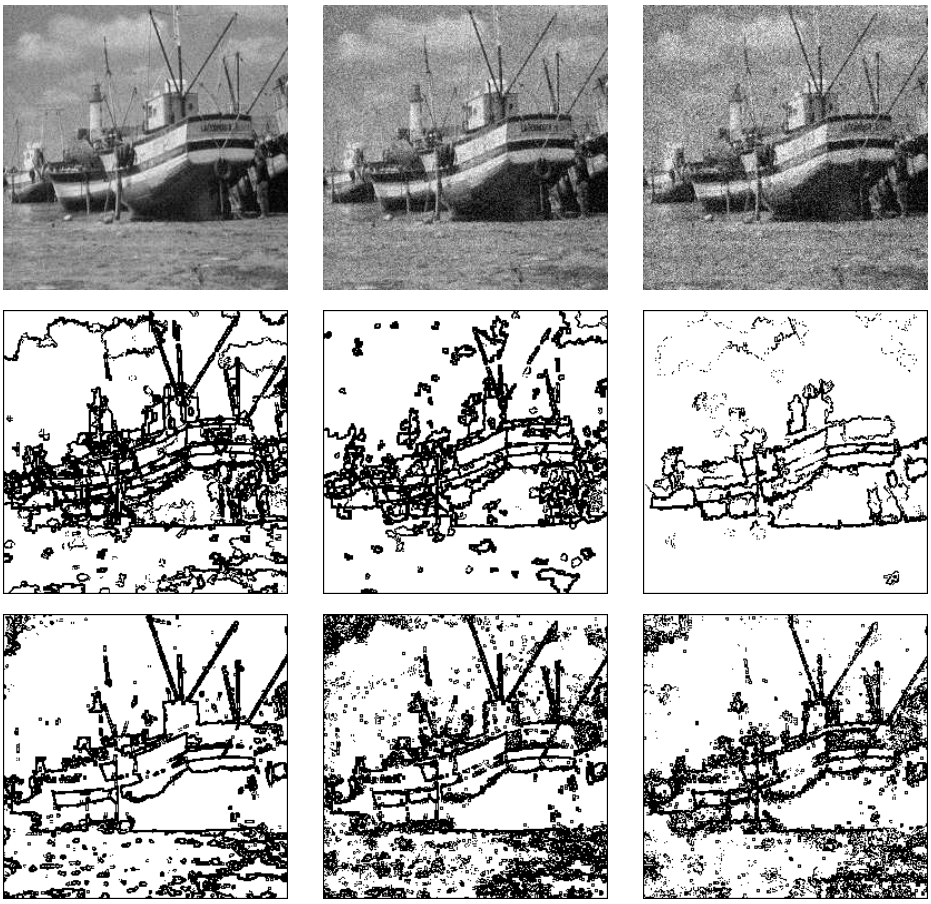

Figure 5.12: Comparative performance of mean shift filter and stochastic bucket algorithm on boat image with 10% noise(first column) and 20% noise(second column)and 30% noise(third column). The input image is in the first row,the edge output for mean shift filter only and in combination with SR is indicated in the second and third rows respectively.

is more noisy than the mean shift filtered output, but for applications where the weak and narrow region detection is important, SR provides a powerful tool.

5.11 Results

The results of the application of SR on the output of the Mean Shift filter to detect weak features in noisy images have been brought out in our paper [95].Thus, the addition of SR to mean shift filter combines the tolerance to noise for gross features that mean shift filter has with the ability to detect weak and narrow regions that SR gives. This complementary approach has further been demonstrated to enhance IR images and medical ultrasound images in our papers [96] and [97]

respectively.

5.12 Conclusions

The significant conclusions emerging from this research work are enlisted below.

1. The concept of combining mean shift filter and stochastic resonance to improve the overall performance when handling noisy images has been introduced. This has been implemented by developing the stochastic bucket algorithm.

2. The performance of the stochastic bucket algorithm has been evaluated on very low contrast and very high noise images. The results indicate better performance than the mean shift filter alone.

3. A mathematical treatment of the application of stochastic resonance to edge detection in the presence of threshold by addition of noise has been carried out using theoretical, empirical and algorithmic study not done earlier.

4. The experiments have indicated that the integration of mean shift filter with stochastic resonance enables the detection of weak features in noisy images which remain undetected using robust techniques. While robust techniques can tolerate noise, they cannot improve weak signals. This is achieved by SR which boosts such signals to cross the detection threshold by addition of noise.

Chapter 6

Conclusions

In the preceding chapters, we described the work done on segmenting noisy images with particular emphasis on the preservation of certain weak features. The work proceeded in two major directions. The performance of the mean shift filter on noisy and low contrast images was investigated systematically. An innovative approach leading to the development of algorithms that go beyond the mean shift filter and with a potential to define a complementary path to robust techniques for segmentation was proposed.

An interesting outcome of the research was the study of segmentation algorithms with respect to image SNR. In this framework, it is possible to classify algorithms into four categories: those that work on images with high signal and low noise (clean images of Category - I), high signal and high noise (noisy images of Category - II), low signal and low noise (low contrast images of Category - III) and low signal and high noise (low contrast and noisy images of Category - IV).

All the segmentation algorithms including the early ones based on thresholding and edge detection work on Category - I images. Most of the research on segmentation is focussed on Category - II as there appears to be an implicit assumption that the signal is detectable despite the presence of noise. Robust techniques, including robust clustering approaches, are the best examples for algorithms that work on Category - II images. Very little work appears in literature on Category - III and Category - IV images although such images routinely figure in civilian surveillance applications (such as CCTV video), military, infra-red photography and radar applications.

Another observation is that there is also an implicit notion of scale in robust

techniques. Scale is a parameter that is loosely related to the features in the image. It is either assumed known or is estimated from the data through parameter estimation. It is felt that this dependence on scale, either implicitly or explicitly, is one of the limitations of the robust techniques on Category III and IV images. For example, robust statistical techniques like LMS and M-estimators need carefully chosen tuning parameters to ensure outlier resistance. The breakdown of MINPRAN, MUSE and ALKS when the amount of noise becomes large has also been studied.

Scale enters Mean Shift algorithm in the form of the two normalization constants. The appropriate values (those that lead to good segmentation) are closely linked to noise and when the noise exceeds 20%, the algorithm breaks down. The breakdown occurs even when explicit dependence on these two constants is removed. Such a result is shown by our experiments on the weighted mean shift and variable bucket extensions to the mean shift filter. In these two variants, "optimal" values are discovered from the data based on the variance in the image data.

The limiting value of 20% noise for mean shift filter seems real in that no variant or selection of parameters resulted in good segmentation. Also, the weak features characterized either by their small size or low contrast are rendered undetectable by the algorithm. This, we conclude, is due to their scale as measured against the normalization constants is too small for them to be signals.

In the thesis, higher amounts of noise are handled by the use of stochastic resonance (SR). SR boosts the signal strength and converts a Category III or IV image into a Category II image. Thus, SR and robust techniques appear to provide a way to handle Category III and IV images. From this perspective, the work in this thesis may be considered the first step towards the development of a new family of algorithms for the hitherto little explored area of segmentation.

Our results show that SR works even on images with 30% and higher noise as well as on weak, barely detectable signals. Thus, it is possible to state that SR may be complementary to robust techniques in that robust techniques are useful in dealing with low SNR signals caused by high noise (with S strong enough to be detectable above a threshold) while SR improves low SNR caused by weak signals.

6.1 Conclusions

The work in this thesis makes two major contributions to the area of segmenting noisy and low contrast images. The first contribution is the systematic study of mean shift filter and its performance on images with varying levels of noise. Mean Shift filter is limited in its performance to images with less than 20% Gaussian noise. On higher amounts of noise, neither the basic filter nor any of its variants produce good performance. Moreover, they also eliminate weak features which may sometimes be important.

The second contribution is the development of novel approach to handling images with high amounts of noise. The novelty lies in viewing certain robust techniques, in particular mean shift filtering, from the perspective of stochastic resonance. We developed an algorithm that combines stochastic resonance with mean shift filtering and the results obtained on nearly 120 images show that the new approaches work on low SNR images where the other techniques begin to fail. Stochastic resonance improved upon mean shift filter in the case of low SNR caused by high noise when the underlying signal is not strong enough to be detectable. Stochastic resonance has also been shown to handle low SNR caused by weak signals (i.e., low contrast images) within the same framework. Finally, we showed that kernel density estimation framework provides the necessary potential well structure which forms the basis for stochastic resonance observed and being exploited by research communities in Physics and Biology.

Other significant results include the performance analysis of mean shift filter and its variants and the creation of a database of 160 images (40 clean and 40 each of images corrupted with 10%, 20% and 30% Gaussian noise) which is useful to researchers in the area of image segmentation. The research has demonstrated mathematically, empirically and practically (by using noisy images) the existence of stochastic resonance phenomenon during the edge detection process. The results also show that stochastic resonance works even on images with 30% and also higher noise content(50% noise) having weak, barely detectable signals. The research convinces that the study of stochastic resonance in computer vision merits greater attention.

6.2 Scope for further work

There is immense scope for robust filtering of images by using the complementary techniques of reducing the effect of noise and boosting the weak signal considering the useful results obtained in detecting weak features in noisy images by using this approach.

The present research work has been carried out on gray scale images. There is scope to develop variants for colored images contaminated with Gaussian noise. Also these algorithms can be studied for their performance on images contaminated with other types of noise (non-Gaussian).

Other areas of Computer Vision like surface fitting and estimation can also be studied using this approach. Such problems can be studied theoretically, empirically and experimentally. Another area of research could be to extend the three-dimensional feature space to a higher dimension feature space by including a variable like time for developing robust algorithms for filtering time varying noisy images (typically found in astronomical images). Finally, an extremely interesting approach would be to modify the equation for the mean shift vector by adding stochastic resonance which provides a mathematically rigorous foundation for handling the complementarity of SR and robust techniques.

Bibliography

[1] Rafael C Gonzalez & Richard E Woods. *Digital Image Processing*. Pearson Education Asia 2002.

[2] Bernd Jahne. Practical Handbook on Image Processing for Scientific and Technical Applications. CRC Press 2004.

[3] Scott E Umbaugh. *Computer Imaging. Digital Image Analysis and Processing*. CRC Press 2005.

[4] John Shawe-Taylor and Nello Cristianini. Kernel Methods for Pattern Analysis. Cambridge University Press 2004.

[5] Peter Meer, Charles V Stewart and David E Tyler. Robust Computer Vision : An Interdisciplinary Challenge. Computer Vision and Image Understanding 78, 1-7 (2000).

[6] Milan Sonka,Vaclav Hlavac & Roger Boyle. Image Processing, Analysis and Machine Vision, 2nd Edition, Brooks/Cole Thomson Learning.

[7] Ale š Leonardis and Horst Bischof *Digital Image Analysis : Selected Techniques and Applications*. Springer-Verlag New York Inc. 2001, pp 219-235.

[8] Charles V Stewart. Robust Parameter Esimation in Computer Vision. SIAM Review 1999, Vol 41,No 3,pp 513-517.

[9] PVC Hough. Method and Means for Recognizing Complex Patterns, United States Patent 3069654, December 18, 1962.

[10] MA Fischler and RC Bolles. Random Sample Consensus : A Paradigm for Model Fitting with Applications to Image Analysis and Automated Cartography. Comm., ACM 24(6) : 381-395, June 1981.

[11] Charles V Stewart. MINPRAN : A New Robust Estimator for Computer Vision. IEEE Trans. on Pattern Anal. Machine Intelligence, 17 (1995) pp 925-938.

[12] J.V.Miller and C.V.Stewart. MUSE : Robust Surface fitting using unbiased scale estimates in Proceedings,IEEE Conference on Computer Vision and Pattern Recognition, 1996, pp 300-306.

[13] K.M.Lee, Peter Meer and R.H.Park. Robust Adaptive Segmentation of Range Images. IEEE Trans. on Pattern Anal. Machine Intelligence, 20(1998) pp 200-205.

[14] P.J.Rousseuw and A.M.Leroy. Robust Regression and Outlier Detection. NY : John Wiley & Sons, 1987.

[15] R.N.Dave. Fuzzy-shell clustering and applications to circle detection in digital images. Int. J. General Syst. Vol. 16, pp 343-355,1990.

[16] R.N Dave and K.Bhaswan. Adaptive fuzzy C-shells clustering and detection of ellipses. IEEE Trans. Neural Networks,vol 3, pp 643-662, May 1992.

[17] R.N.Dave and K.J.Patel. Progressive fuzzy clustering algorithms for for characteristic shape recognition in Proc. NAFIPS 90 : Quarter Century of Fuzziness, I.B.Turksen, Ed., June 1990,vol. I,pp 121-124.

[18] I. Gath and Y Man. Detection and Separation of ring-shaped clusters using fuzzy clustering. IEEE Trans. Pattern Anal.Machine Intelligence. Vol. 16, pp 855-861, Aug 1994.

[19] R.Krishnapuram, H.Frigui and O.Nasraoui. Quadric shell clustering algorithms and their applications. Pattern Recogn. Letters, vol14,no 7,pp 545-552, July 1993.

[20] R.Krisnapuram,H.Frigui and O.Nasraoui.Fuzzy and possibilistic shell clustering algorithms and their application to boundary detection and surface approximation : Parts I and II. IEEE Trans. Fuzzy Syst., vol.3, pp29-60, Feb 1995.

[21] R. Krishnapuram, O. Nasraoui, and H. Frigui, Fuzzy C spherical shells algorithm: A new approach," IEEE Trans. Neural Networks, vol. 3, pp. 663-671, Sept. 1992.

[22] R.N.Dave. Characterization and detection of noise in clustering. Pattern Recognition Lett., vol. 12, no. 11, pp. 657-664, 1991.

[23] R.N.Dave Robust fuzzy clustering algorithms in 2nd IEEE Int. Conf. Fuzzy Syst., San Francisco, CA, Mar. 28-Apr. 1,1993, pp. 1281-1286.

[24] J. J. De Gruijter and A. B. McBratney. A modified fuzzy K-means method for predictive classification. in Classification and Related Methods of Data Analysis, H. H. Bock, Ed. Amsterdam, The Netherlands: Elsevier, 1988.

[25] J.-M. Jolion, P. Meer, and S. Bataouche. Robust clustering with applications in computer vision. IEEE Trans. Pattern Anal. Machine Intell., vol. 13, pp. 791-802, Aug. 1991.

[26] R. Krishnapuram and J. M. Keller. A possibilistic approach to clustering . IEEE Trans. Fuzzy Syst., vol. 1, pp. 98-110, May 1993.

[27] Y. Ohashi, "Fuzzy clustering and robust estimation," in 9th Meet. SAS Users Grp. Int., Hollywood Beach, FL, 1984.

[28] X. Zhuang, Y. Huang, K. Palaniappan, and Y. Zhao. Gaussian mixture density modeling, decomposition and Applications. IEEE Trans. Image Processing, vol. 5, pp. 1293-1302, Sept. 1996.

[29] AK Jain and RC Dubes. Algorithms for Clustering Data. Englewood Cliffs NJ. Prentice Hall 1988.

[30] Earl Gose,Richard Johnsonbaugh and Steve Jost. Pattern Recognition and Image Analysis. Prentice Hall of India. New Delhi 1999.

[31] J.T.Tou and R.C.Gonzales. Pattern Recognition Principles. Reading,MA Addison-Wesley 1974.

[32] S.Chiu and JJ Cheng. Automatic rule generation of fuzzy rule base for robot arm posture selection in Proc. NAFIPS Conf., San Antonio, TX,Dec 1994,pp 436- 440.

[33] RR Yager and DP Filev. Approximate clustering via the mountain method. IEEE Trans. Syst. Man, Cybern., vol 24, pp 1279-1284, Aug 1994

[34] K.Rose, E.Gurewitz and GC Fox. A Deterministic Annealing approach to Clustering. Pattern Recogn.Lett., vol. 11, pp. 589-594, Sept 1990.

[35] R.M.Haralick and L.G.Shapiro. Computer and Robot Vision. Reading,MA Addison-Wesley, 1992,vol.I, ch.11.

[36] D.G.Lowe. Fitting parametrized three-dimensional models to images. IEEE Trans. Pattern Anal. Machine Intell, vol.13, pp441-450, May 1991.

[37] P.Whaite and F.P. Ferrie. From Uncertainty to Visual Exploration. IEEE Trans. Pattern Anal. Machine Intell., vol.13, pp 1038-1049, Oct 1991.

[38] H.Frigui and R. Krishnapuram. A Robust Competitive Clustering Algorithm with Applications in Computer Vision. IEEE Trans. on Pattern Anal. Machine Intell., Vol 21, No. 5, May 1999.

[39] R.N.Dave and R.Krishnapuram. Robust Clustering Methods : A Unified View. IEEE Trans. on Fuzzy Systems, vol. 5, no., 2 May 1997, pp 270-293.

[40] Wikipedia-Stochastic Resonance available at http://en.wikipedia.org/wiki/Stochastic_resonance

[41] P.J.Huber, Robust Statistics, John Wiley, New York, 1981.

[42] F.R.Hampel, P.J.Rousseeuw, E Ronchetti and W.A.Stahel, Robust Statistics : The Approach Based on Influence Functions, John Wiley, New York, 1986.

[43] Benzi R, A Sutera and A Vulpiani. The Mechanism of Stochastic Resonance, J. Physics A14 , L453 (1981).

[44] Benzi R, G Parisi, A Sutera and A Vulpiani. Stochastic resonance in climatic change, Tellus V 34 (10), (1982).

[45] Benzi R, A Sutera, G Parisi and A Vulpiani. A Theory of Stochastic Resonance in Climate Change, SIAM (Soc. Ind. Appl. Math) J Appl Math 43, 565 (1983).

[46] Nicolis, C., 1981, Sol. Phys. 74, 473.

[47] Nicolis, C., 1982, Tellus 34, 1.

[48] Nicolis, C., 1993, J. Stat. Phys. 70, 3.

[49] Nicolis, C., and G. Nicolis, 1981, Tellus 33, 225.

[50] Nicolis, C., G. Nicolis, and G. Hu, 1990, Phys. Lett. A 151, 139.

[51] Fauve, S. and F.Heslot. Stochastic Resonance in a bistable system, Phys Lett. 97A,5 (1983).

[52] McNamara,B., K.Wiesenfeld, and R.Roy, 1988, Phys. Rev. Lett. 60, 2626

[53] Bruno Ando, SalvatoreGraziani(Editors).Stochastic Resonance Theory and Applications, Kluwer Academic Publishers,2000

[54] Adi R Bulsara,Luca Gammaitoni.Tuning in to noise.Physics Today,March 1996.

[55] Luca Gammaitoni,Peter Hanggi,Peter Jung and Fabio Marchesoni.Stochastic resonance.Reviews of Modern Physics, Vol. 70, No. 1, January 1998

[56] Francois Chapeau-Blondeau.Stochastic Resonance and Optimal Detection of Pulse Trains by Threshold Devices.Digital Signal Processing 9, 162177 (1999).

[57] Donatella Petracchi,Ilse C. Gebeshuber,Louis J. DeFelice and Arun V. Holden. Stochastic resonance in biological systems.Chaos, Solitons and Fractals 11 (2000) 1819-1822

[58] Donatella Petracchi.What is the role of stochastic resonance? Chaos, Solitons and Fractals 11 (2000) 1827-1834.

[59] Z. Gingl, R. Vajtai and L.B. Kiss. Signal-to-noise ratio gain by stochastic resonance in a bistable system.Chaos, Solitons and Fractals 11(2000) 1929-1932.

[60] Steeve Zozor and Pierre-Olivier Amblard. On the use of stochastic resonance in sine detection.Signal Processing 82 (2002) 353 367.

[61] Peter Babinec.Stochastic resonance in an interacting-agent model of stock market.Chaos, Solitons and Fractals 13 (2002) 17671770.

[62] Bohou Xu,Fabing Duan,Ronghao Bao and Jianlong Li. Stochastic resonance with tuning system parameters : The application of bistable systems in signal processing.Chaos, Solitons and Fractals 13 (2002) 633-644.

[63] Aditya A. Saha and G.V. Anand.Design of detectors based on stochastic resonance.Signal Processing 83 (2003) 1193 1212.

[64] Bart Koskoa and Sanya Mitaimb.Stochastic resonance in noisy threshold neurons.Neural Networks 16 (2003 Special Issue) pp 755-761.Elsevier.

[65] Hu Niaoqing, Chen Min and Wen Xisen.The application of stochastic resonance theory for early detecting rub-impact fault of rotorsystem.Mechanical Systems and Signal Processing (2003) 17(4), pp 883-895. Elsevier.

[66] Fan Zhang, Lan Chen, Yan-Ni Li, Ben-Xiang Wu, Zun-Sheng Cai and Xue-Zhuang Zhao.The influence of potential to stochastic resonance in model system of bistable states chemical reaction.Chaos, Solitons and Fractals 15 (2003) pp 679-685.

[67] Ashok Patel and Bart Kosko.Stochastic resonance in noisy spiking retinal and sensory neuron models.Neural Networks 18 (2005 Special Issue)pp 467-478

[68] Barney E. Klamecki.Use of stochastic resonance for enhancement of low-level vibration signal components.Mechanical Systems and Signal Processing 19 (2005) pp 223-237.Elsevier.

[69] David Rousseau, Franois Chapeau-Blondeau.Stochastic resonance and improvement by noise in optimal detection strategies.Digital Signal Processing 15 (2005) pp 19-32.Elsevier.

[70] Yong-gang Lenga,Tai-yong Wanga,Yan Guob,Yong-gang Xua and Sheng-bo Fan.Engineering signal processing based on bistable stochastic resonance.Mechanical Systems and Signal Processing 21 (2007) pp 138-150.(Available at www.sciencedirect.com)

[71] Bohou Xua,Lingzao Zenga and Jianlong Li.Application of stochastic resonance in target detection in shallow-water reverberation.Journal of Sound and Vibration 303 (2007) 255263.(Available at www.sciencedirect.com)

[72] D Comaniciu and P Meer. Mean Shift Analysis and Applications,Proc. of the Seventh IEEE Intl. Conference on Computer Vision (ICCV99) Vol 2, Pages : 1197-1203

[73] D Comaniciu and P Meer, Mean Shift: A Robust Approach Toward Feature Space Analysis,IEEE Trans. on Pattern Analysis and Machine Intelligence, Vol 24, No 5 ,May 2002. Pages : 603-619.

[74] M Herbin, N Bonnet and P Vantrot, A Clustering Method Based on the Estimation of the Probability Density Function and on the Skeleton by Influence zones. Pattern Recognition Letters, vol 17, pp 1141-1150, 1996.

[75] A Touzani and J G Postaire, Clustering by Mode Boundary Detection. Pattern Recognition Letters, Vol 9, pp 1-12, 1989.

[76] R Wilson and M Spann, A New Approach to Clustering. Pattern Recognition, Vol 23, pp 1413-1425, 1990.

[77] Wendy L Martinez and Angel R Martinez. Computational Statistics Handbook with MATLAB. Chapman & Hall/CRC 2002.

[78] Epanechnikov V.A, Non-parametric estimation of a multivariate probability density. Theory Probab. Appl.14 pp 153-158.

[79] Silverman B.W. Density Estimation for Statistics and Data Analysis. Chapman & Hall,1986.

[80] D.W.Scott. Multivariate Density Estimation Theory Practice and Visualization. Wiley 1992.

[81] Qinghua Ye, Haining Huang and Chunhua Zhang.Image enhancement using stochastic resonance. International Conference on Image Processing,2004(ICIP2004).

[82] Rajib Kumar Jha, P.K.Biswas and B.N.Chatterji. Image Denoising using Stochastic Resonance. Proc. of the Intl.Conference on Cognition and Recognition, Mysore, India, 2005

[83] Winbing Tao,Y.Z., and Hai Jin, Color Image Segmentation based on Mean Shift and Normalized Cuts, IEEE Trans. Systems,Man and Cybernetics,37.1382-1389, Oct 2007.

[84] K. Wiesenfeld, T. Wellens, and A. Buchleitner. Coherent Evolution in Noisy Environments, Springer, Berlin, 2002.

[85] T. Wellens, V. Shatokhin and A. Buchleitner. Stochastic Resonance, Rep. Prog. Phys., 67(1),pp. 45–105, 2004.

[86] J. Casado-Pascual, J. Gomez-Ordonez and M. Morillo. Stochastic Resonance: theory and numerics, Chaos 15, 2005.

[87] Priscilla E Greenwood, Ursulla U Muller, Lawrence M Ward and Wolfgang Wefelmeyer. Statistical Analysis of Stochastic Resonance in a Thresholded Detector, Austrian Journal of Statistics, vol.32 Number 1(2) ,pp. 49–70, 2003.

[88] U. U. Müller. Nonparametric regression for threshold data. Canadian Journal of Statistics, 28:301310, 2000.

[89] John F. Canny. A Theory of Edge Detection, IEEE Trans. on Pattern Analysis and Machine Intelligence, 1986.

[90] D.W. Repperger and K.A. Farris.Stochastic resonance a nonlinear control theory interpretation.International Journal of Systems Science Vol. 41, No. 7, July 2010, 897907

[91] Choonwoo Ryu, Seong G.Kong and Hakil Kim. Enhancement of feature extraction for low-quality fingerprint images using stochastic resonance.Pattern Recognition Letters 32(2011), 107-113.

[92] Qingbo He and Jun Wang.Effects of multiscale noise tuning on stochastic resonance for weak signal detection.Digital Signal Processing 22(2012), 614-621.

[93] Qingbo He,JunWang,YongbinLiu,DaoyiDai and FanrangKong.Multiscale noise tuning of stochastic resonance for enhanced fault diagnosis in rotating machines.Mechanical Systems and Signal Processing 28(2012),443-457

[94] V.N. Hari,G.V.Anand,A.B.Premkumar and A.S.Madhukumar.Design and performance analysis of a signal detector based on suprathreshold stochastic resonance.Signal Processing 92(2012)1745-1757.

[95] J V R Sagar and Bhagvati Chakravarthy. Stochastic Resonance and Mean Shift Filtering for Detecting Weak Features in Noisy Images.International Conference on Signal and Image Processing (ICSIP2012). Springer Lecture Notes in Electrical Engg.

[96] J V R Sagar and Bhagvati Chakravarthy. Stochastic Resonance and Mean Shift Filtering : A Complementary Approach for detecting weak feature in noisy IR images. (communicated to Defence Science Journal, DRDO, New Delhi in May 2013)

[97] J V R Sagar and Bhagvati Chakravarthy. Stochastic Resonance aided Robust Techniques for Segmentation of Medical Ultrasound Images. (communicated to NCVPRIPG 2013 in Aug 2013)

Appendix A

Results of Experiments

The results obtained by the use of the mean shift filter, weighted mean shift filter, variable bucket size mean shift filter and SR based mean shift filter (stochastic bucket algorithm) are given in the tables included in this appendix. The test image database used has 160 images. It consists of 40 original images and 120 noisy images obtained by contaminating the original images with Gaussian noise of σ of 10%, 20% and 30%. The images are of different types with low/high number of regions and low/high intensity variations. The values of the normalization constants σ_s and σ_r used for filtering the images are those which give the highest value of the PSNR when the mean shift filter is used. The filtered output is measured quantitatively in terms of three measures (i) PSNR (ii) region count and (iii) Pratts figure-of-merit for the edge quality in the output image.

The effect of the normalization constants on the filter output is evident for the mean shift filter in the presence of noise of up to 20%. The filter fails to segment the image when the noise is increased beyond 20% and the results for 30% noise is not given. The results show that there are no significant improvements for the weighted mean shift filter. This is because the noise that is present in these images is not localized to any particular region of the image. However, in the variable bucket size filter, more number of regions get segmented than the basic mean shift filter even when there is 20% Gaussian noise.

Finally, in the case of SR based mean shift filter it is observed that even for the high noise case of 30% Gaussian noise also, more regions get detected. Where the region count is less, the edge quality is superior as measured by Pratts figure-of-merit. The complementary approach of using mean shift filter to reduce the

effect of noise and stochastic resonance to boost the weak signal in the image to improve the SNR is demonstrated by these results.

Table A.1: Results of mean shift filtering

S.No.	Image	Gaussian Noise	σ_s	σ_r	PSNR	Region Count	Pratts Fig-of-merit
1	cameraman	nil	1	1	54.06	1053	0.86
		10%	8	4	34.02	713	0.87
		20%	8	8	28.59	362	0.82
2	peppers	nil	1	1	54.39	732	0.87
		10%	4	4	29.72	748	0.83
		20%	4	8	25.30	398	0.82
3	mandrill	nil	1	1	54.34	1860	0.86
		10%	1	1	28.19	2413	0.83
		20%	4	4	22.47	1457	0.82
4	lena	nil	1	1	54.33	735	0.82
		10%	4	4	31.01	615	0.79
		20%	4	8	27.15	264	0.77
5	boat	nil	1	1	55.47	973	0.86
		10%	4	4	30.70	747	0.80
		20%	4	8	25.89	379	0.72
6	flower	nil	1	1	54.12	303	0.45
		10%	4	4	31.73	484	0.73
		20%	4	8	27.11	158	0.37
7	oranges	nil	1	1	54.22	566	0.57
		10%	2	4	30.08	747	0.79
		20%	8	4	23.99	744	0.76
8	cactus	nil	1	1	54.40	953	0.80
		10%	4	4	31.39	859	0.80
		20%	8	4	24.83	1182	0.77
9	duck	nil	1	1	53.82	187	0.69
		10%	4	4	35.59	269	0.79
		20%	4	8	30.12	174	0.75
10	bridge	nil	1	1	51.18	1244	0.67
		10%	4	4	37.90	840	0.72
		20%	4	8	32.78	470	0.69

Table A.2: Results of mean shift filtering(contd..)

S.No.	Image	Gaussian Noise	σ_s	σ_r	PSNR	Region Count	Pratts Fig-of-merit
11	tank	nil	1	1	55.22	287	0.56
		10%	2	4	30.00	327	0.40
		20%	4	4	23.90	580	0.66
12	butterfly	nil	1	1	54.91	527	0.18
		10%	4	4	32.96	618	0.72
		20%	4	8	29.81	467	0.67
13	cat	nil	1	1	53.85	1330	0.77
		10%	4	4	28.58	716	0.76
		20%	8	4	23.48	1001	0.71
14	barbara	nil	1	1	54.25	1283	0.61
		10%	2	4	28.67	1376	0.61
		20%	4	4	22.94	1628	0.60
15	flintstones	nil	1	1	54.19	1064	0.89
		10%	2	4	29.02	1253	0.89
		20%	2	8	23.28	1022	0.86
16	clock	nil	1	1	54.92	152	0.59
		10%	4	4	32.20	285	0.69
		20%	4	8	26.92	308	0.73
17	fruits	nil	1	1	51.99	920	0.74
		10%	2	4	29.80	1307	0.85
		20%	4	8	24.62	651	0.76
18	grapes	nil	1	1	54.11	2723	0.82
		10%	1	1	28.31	2929	0.80
		20%	4	4	22.56	2384	0.79
19	house	nil	1	1	56.43	367	0.65
		10%	4	4	32.98	297	0.54
		20%	4	8	28.77	178	0.58
20	Plane	nil	1	1	53.55	68	0.24
		10%	2	4	30.24	260	0.62
		20%	4	8	30.72	108	0.43

Table A.3: Results of mean shift filtering(contd..)

S.No.	Image	Gaussian Noise	σ_s	σ_r	PSNR	Region Count	Pratts Fig-of-merit
21	Plant	nil	1	1	53.37	1813	0.82
		10%	4	4	28.98	1398	0.79
		20%	4	8	24.79	531	0.79
22	Scene1	nil	1	1	53.50	1294	0.88
		10%	4	4	30.88	1490	0.85
		20%	4	8	25.50	1092	0.82
23	Shark	nil	1	1	53.44	64	0.41
		10%	2	4	33.13	234	0.62
		20%	4	8	32.27	57	0.49
24	Ship	nil	1	1	53.26	1319	0.79
		10%	4	4	30.78	1213	0.78
		20%	4	8	25.09	822	0.73
25	Shore	nil	1	1	53.67	1177	0.85
		10%	4	4	29.74	988	0.83
		20%	4	8	24.77	564	0.79
26	Copter	nil	1	1	54.24	742	0.82
		10%	4	4	31.67	866	0.80
		20%	4	8	26.54	537	0.69
27	Brodatz	nil	1	1	54.39	1040	0.83
		10%	2	4	28.69	1196	0.77
		20%	4	8	23.91	358	0.79
28	Scene2	nil	1	1	54.64	1730	0.74
		10%	4	4	30.82	1337	0.75
		20%	4	8	25.88	732	0.69
29	Scene3	nil	1	1	54.41	1287	0.76
		10%	4	4	34.62	1018	0.70
		20%	4	8	30.38	491	0.71
30	Scene4	nil	1	1	54.21	864	0.85
		10%	4	4	32.11	899	0.83
		20%	4	8	27.79	673	0.75

Table A.4: Results of mean shift filtering(contd..)

S.No.	Image	Gaussian Noise	σ_s	σ_r	PSNR	Region Count	Pratts Fig-of-merit
31	Scene5	nil	1	1	53.27	1222	0.85
		10%	4	4	31.32	1009	0.83
		20%	4	8	26.08	691	0.76
32	Scene6	nil	1	1	54.39	1457	0.79
		10%	4	4	30.57	835	0.81
		20%	8	4	24.81	989	0.72
33	Scene7	nil	1	1	54.28	2161	0.84
		10%	4	4	29.66	1414	0.83
		20%	8	4	24.07	1739	0.74
34	Space1	nil	1	1	55.07	681	0.71
		10%	2	4	30.12	850	0.75
		20%	4	8	26.59	308	0.68
35	Space2	nil	1	1	55.64	1442	0.88
		10%	4	2	29.06	1935	0.84
		20%	4	8	23.55	760	0.74
36	Tree	nil	1	1	55.72	1417	0.87
		10%	4	4	31.08	825	0.86
		20%	4	8	26.29	414	0.65
37	Vegetables	nil	1	1	53.87	1779	0.86
		10%	1	1	28.31	2674	0.81
		20%	2	8	23.45	1245	0.81
38	Bird	nil	1	1	52.89	248	0.65
		10%	4	4	34.62	301	0.82
		20%	8	8	29.80	109	0.78
39	Barco	nil	1	1	54.59	512	0.82
		10%	4	4	30.94	700	0.72
		20%	4	8	27.44	347	0.69
40	Lizard	nil	1	1	53.60	1338	0.68
		10%	4	4	32.25	1167	0.66
		20%	4	8	27.81	676	0.68

Table A.5: Results of median shift filtering for sample images

S.No.	Image	Gaussian Noise	σ_s	σ_r	PSNR	Region Count	Pratts Fig-of-merit
1	cameraman	10%	8	4	28.02	965	0.75
		20%	8	8	22.19	745	0.69
2	peppers	10%	4	4	26.62	1130	0.77
		20%	4	8	21.15	751	0.74
3	lena	10%	4	4	27.01	999	0.69
		20%	4	8	21.40	718	0.66

Table A.6: Results of weighted mean shift filtering

S.No.	Image	Gaussian Noise	σ_s	σ_r	PSNR	Region Count	Pratts Fig-of-merit
1	cameraman	10%	8	4	34.06	714	0.87
		20%	8	8	28.59	361	0.82
2	peppers	10%	4	4	29.75	759	0.83
		20%	4	8	25.28	396	0.82
3	mandrill	10%	1	1	28.19	2413	0.83
		20%	4	4	22.46	1473	0.82
4	lena	10%	4	4	31.01	615	0.79
		20%	4	8	27.06	266	0.77
5	boat	10%	4	4	30.72	756	0.80
		20%	4	8	25.92	380	0.72
6	flower	10%	4	4	31.60	473	0.75
		20%	4	8	26.97	161	0.37
7	oranges	10%	2	4	30.03	758	0.78
		20%	8	4	23.97	747	0.76
8	cactus	10%	4	4	31.38	869	0.80
		20%	8	4	24.79	1184	0.77
9	duck	10%	4	4	35.44	282	0.79
		20%	4	8	29.83	173	0.75
10	bridge	10%	4	4	37.85	850	0.72
		20%	4	8	32.72	477	0.69
11	tank	10%	2	4	29.98	344	0.41
		20%	4	4	23.84	586	0.64
12	butterfly	10%	4	4	32.91	617	0.72
		20%	4	8	29.81	463	0.67
13	cat	10%	4	4	28.60	732	0.76
		20%	8	4	23.46	1002	0.71
14	barbara	10%	2	4	28.67	1366	0.61
		20%	4	4	22.92	1628	0.60

Table A.7: Results of weighted mean shift filtering(contd..)

S.No.	Image	Gaussian Noise	σ_s	σ_r	PSNR	Region Count	Pratts Fig-of-merit
15	flintstones	10%	2	4	29.04	1276	0.89
		20%	2	8	23.31	1046	0.85
16	clock	10%	4	4	32.30	286	0.70
		20%	4	8	26.91	315	0.72
17	fruits	10%	2	4	29.79	1335	0.86
		20%	4	8	24.60	658	0.77
18	grapes	10%	1	1	28.31	2929	0.80
		20%	4	4	22.56	2399	0.79
19	house	10%	4	4	33.03	299	0.54
		20%	4	8	28.67	178	0.58
20	Plane	10%	2	4	30.20	259	0.62
		20%	4	8	30.65	108	0.43
21	Plant	10%	4	4	28.96	1394	0.79
		20%	4	8	24.73	536	0.79
22	Scene1	10%	4	4	30.91	1492	0.85
		20%	4	8	25.54	1105	0.82
23	Shark	10%	2	4	32.76	248	0.63
		20%	4	8	31.73	54	0.49
24	Ship	10%	4	4	30.80	1211	0.78
		20%	4	8	25.18	826	0.73
25	Shore	10%	4	4	29.77	987	0.83
		20%	4	8	24.74	581	0.79
26	Copter	10%	4	4	31.72	866	0.81
		20%	4	8	26.48	539	0.71
27	Brodatz	10%	2	4	28.70	1178	0.77
		20%	4	8	23.97	362	0.79
28	Scene2	10%	4	4	30.91	1348	0.75
		20%	4	8	25.88	738	0.69

Table A.8: Results of weighted mean shift filtering(contd..)

S.No.	Image	Gaussian Noise	σ_s	σ_r	PSNR	Region Count	Pratts Fig-of-merit
29	Scene3	10%	4	4	34.60	1027	0.70
		20%	4	8	30.23	494	0.71
30	Scene4	10%	4	4	32.11	896	0.82
		20%	4	8	27.73	681	0.75
31	Scene5	10%	4	4	31.30	1014	0.82
		20%	4	8	26.01	695	0.76
32	Scene6	10%	4	4	30.56	840	0.81
		20%	8	4	24.79	983	0.72
33	Scene7	10%	4	4	29.68	1418	0.82
		20%	8	4	24.06	1743	0.74
34	Space1	10%	2	4	30.13	850	0.75
		20%	4	8	26.55	313	0.66
35	Space2	10%	4	2	29.07	1931	0.84
		20%	4	8	23.55	753	0.72
36	Tree	10%	4	4	31.07	825	0.86
		20%	4	8	26.25	411	0.64
37	Vegetables	10%	1	1	28.31	2674	0.81
		20%	2	8	23.42	1240	0.81
38	Bird	10%	4	4	34.43	299	0.82
		20%	8	8	29.71	109	0.79
39	Barco	10%	4	4	30.92	700	0.72
		20%	4	8	27.34	352	0.69
40	Lizard	10%	4	4	32.15	1163	0.66
		20%	4	8	27.67	684	0.68

Table A.9: Results of variable bucket size mean shift filtering

S.No.	Image	Gaussian Noise	σ_s	σ_r	PSNR	Region Count	Pratts Fig-of-merit
1	cameraman	10%	256	4	33.24	963	0.87
		20%	256	8	28.92	484	0.81
2	peppers	10%	256	4	29.38	783	0.84
		20%	256	8	24.78	398	0.81
3	mandrill	10%	256	1	28.19	2365	0.83
		20%	256	4	22.28	1588	0.83
4	lena	10%	256	4	30.13	726	0.77
		20%	256	8	26.23	272	0.78
5	boat	10%	256	4	30.44	852	0.79
		20%	256	8	25.57	395	0.70
6	flower	10%	256	4	30.52	513	0.77
		20%	256	8	26.07	98	0.27
7	oranges	10%	256	4	28.97	602	0.73
		20%	256	4	23.71	910	0.77
8	cactus	10%	256	4	31.44	1013	0.79
		20%	256	4	24.73	1513	0.80
9	duck	10%	256	4	33.22	267	0.80
		20%	256	8	28.99	148	0.70
10	bridge	10%	256	4	36.15	912	0.67
		20%	256	8	28.54	425	0.70
11	tank	10%	256	4	29.18	222	0.36
		20%	256	4	24.16	451	0.49
12	butterfly	10%	256	4	31.13	641	0.72
		20%	256	8	27.48	541	0.54
13	cat	10%	256	4	28.00	855	0.75
		20%	256	4	22.92	1349	0.71
14	barbara	10%	256	4	28.20	1193	0.61
		20%	256	4	22.95	1614	0.60

Table A.10: Results of variable bucket size mean shift filtering(contd..)

S.No.	Image	Gaussian Noise	σ_s	σ_r	PSNR	Region Count	Pratts Fig-of-merit
15	flintstones	10%	256	4	29.08	1146	0.89
		20%	256	8	23.30	794	0.79
16	clock	10%	256	4	32.49	303	0.67
		20%	256	8	27.77	322	0.74
17	fruits	10%	256	4	30.01	1178	0.85
		20%	256	8	24.86	530	0.77
18	grapes	10%	256	1	28.29	2963	0.80
		20%	256	4	22.44	2545	0.79
19	house	10%	256	4	32.96	346	0.58
		20%	256	8	28.20	182	0.58
20	Plane	10%	256	4	34.72	94	0.29
		20%	256	8	31.28	72	0.33
21	Plant	10%	256	4	28.26	1583	0.78
		20%	256	8	23.87	587	0.80
22	Scene1	10%	256	4	30.35	1501	0.85
		20%	256	8	25.15	616	0.83
23	Shark	10%	256	4	37.06	101	0.46
		20%	256	8	33.29	60	0.48
24	Ship	10%	256	4	30.73	1290	0.79
		20%	256	8	25.01	448	0.70
25	Shore	10%	256	4	29.63	1061	0.83
		20%	256	8	24.49	504	0.73
26	Copter	10%	256	4	31.15	831	0.84
		20%	256	8	26.28	315	0.73
27	Brodatz	10%	256	4	28.54	913	0.81
		20%	256	8	23.84	460	0.79
28	Scene2	10%	256	4	30.43	1484	0.76
		20%	256	8	26.08	586	0.65

Table A.11: Results of variable bucket size mean shift filtering(contd..)

S.No.	Image	Gaussian Noise	σ_s	σ_r	PSNR	Region Count	Pratts Fig-of-merit
29	Scene3	10%	256	4	32.66	1196	0.69
		20%	256	8	28.89	587	0.67
30	Scene4	10%	256	4	30.65	1014	0.83
		20%	256	8	25.65	635	0.77
31	Scene5	10%	256	4	31.23	1143	0.83
		20%	256	8	25.84	650	0.75
32	Scene6	10%	256	4	30.34	947	0.80
		20%	256	4	24.50	1307	0.71
33	Scene7	10%	256	4	29.66	1574	0.82
		20%	256	4	23.93	1935	0.74
34	Space1	10%	256	4	29.16	690	0.78
		20%	256	8	25.58	303	0.53
35	Space2	10%	256	2	29.06	1932	0.87
		20%	256	8	23.56	800	0.78
36	Tree	10%	256	4	31.03	1024	0.86
		20%	256	8	25.56	556	0.69
37	Vegetables	10%	256	1	28.30	2663	0.81
		20%	256	8	22.50	787	0.84
38	Bird	10%	256	4	34.28	299	0.84
		20%	256	8	29.67	155	0.79
39	Barco	10%	256	4	29.49	659	0.71
		20%	256	8	25.41	265	0.68
40	Lizard	10%	256	4	31.17	1245	0.66
		20%	256	8	26.61	669	0.67

Table A.12: Results of stochastic resonance based mean shift filtering

S.No.	Image	Gaussian Noise	σ_s	σ_r	PSNR	Region Count	Pratts Fig-of-merit
1	cameraman	10%	2,8	2,8	23.15	424	0.80
		20%	2,8	2,8	21.28	592	0.78
		30%	2,8	2,8	23.05	697	0.68
2	peppers	10%	2,8	2,8	21.73	558	0.79
		20%	2,8	2,8	22.74	595	0.81
		30%	2,8	2,8	18.03	714	0.79
3	mandrill	10%	2,8	2,8	19.08	702	0.05
		20%	2,8	2,8	21.03	913	0.45
		30%	2,8	2,8	18.01	1171	0.16
4	lena	10%	2,8	2,8	20.40	400	0.79
		20%	2,8	2,8	20.86	473	0.76
		30%	2,8	2,8	25.19	559	0.77
5	boat	10%	2,8	2,8	22.24	528	0.70
		20%	2,8	2,8	24.10	134	0.73
		30%	2,8	2,8	21.52	282	0.40
6	flower	10%	2,8	2,8	23.75	547	0.34
		20%	2,8	2,8	18.16	30	0.72
		30%	2,8	2,8	25.43	44	0.41
7	oranges	10%	2,8	2,8	21.63	449	0.43
		20%	2,8	2,8	19.89	184	0.49
		30%	2,8	2,8	20.83	812	0.59
8	cactus	10%	2,8	2,8	17.14	630	0.64
		20%	2,8	2,8	18.03	448	0.54
		30%	2,8	2,8	23.34	952	0.75
9	duck	10%	2,8	2,8	25.81	203	0.69
		20%	2,8	2,8	22.12	41	0.65
		30%	2,8	2,8	20.54	89	0.65
10	bridge	10%	2,8	2,8	20.53	503	0.65
		20%	2,8	2,8	26.87	80	0.65
		30%	2,8	2,8	25.26	517	0.66

Table A.13: Results of stochastic resonance based mean shift filtering(contd..)

S.No.	Image	Gaussian Noise	σ_s	σ_r	PSNR	Region Count	Pratts Fig-of-merit
11	tank	10%	2,8	2,8	20.50	90	0.07
		20%	2,8	2,8	22.87	171	0.05
		30%	2,8	2,8	26.28	267	0.10
12	butterfly	10%	2,8	2,8	23.08	628	0.63
		20%	2,8	2,8	22.70	564	0.65
		30%	2,8	2,8	13.61	807	0.45
13	cat	10%	2,8	2,8	21.33	378	0.56
		20%	2,8	2,8	22.18	174	0.73
		30%	2,8	2,8	20.22	102	0.38
14	barbara	10%	2,8	2,8	21.11	563	0.61
		20%	2,8	2,8	22.77	360	0.61
		30%	2,8	2,8	22.96	174	0.61
15	flintstones	10%	2,8	2,8	14.94	1025	0.58
		20%	2,8	2,8	19.77	298	0.64
		30%	2,8	2,8	18.31	182	0.75
16	clock	10%	2,8	2,8	25.96	481	0.76
		20%	2,8	2,8	22.73	168	0.79
		30%	2,8	2,8	21.15	153	0.76
17	fruits	10%	2,8	2,8	20.77	839	0.61
		20%	2,8	2,8	22.49	509	0.68
		30%	2,8	2,8	15.33	304	0.71
18	grapes	10%	2,8	2,8	19.61	1894	0.85
		20%	2,8	2,8	20.45	1970	0.83
		30%	2,8	2,8	19.62	632	0.84
19	house	10%	2,8	2,8	19.37	236	0.76
		20%	2,8	2,8	24.32	110	0.58
		30%	2,8	2,8	25.22	60	0.48
20	Plane	10%	2,8	2,8	26.87	64	0.38
		20%	2,8	2,8	17.56	42	0.62
		30%	2,8	2,8	28.74	21	0.31

Table A.14: Results of stochastic resonance based mean shift filtering(contd..)

S.No.	Image	Gaussian Noise	σ_s	σ_r	PSNR	Region Count	Pratts Fig-of-merit
21	Plant	10%	2,8	2,8	24.37	1207	0.83
		20%	2,8	2,8	21.21	258	0.65
		30%	2,8	2,8	23.22	241	0.78
22	Scene1	10%	2,8	2,8	19.77	708	0.80
		20%	2,8	2,8	21.33	157	0.84
		30%	2,8	2,8	16.94	93	0.81
23	Shark	10%	2,8	2,8	27.41	27	0.44
		20%	2,8	2,8	19.35	38	0.59
		30%	2,8	2,8	17.29	24	0.59
24	Ship	10%	2,8	2,8	17.68	530	0.42
		20%	2,8	2,8	21.59	189	0.67
		30%	2,8	2,8	19.30	145	0.58
25	Shore	10%	2,8	2,8	16.72	131	0.65
		20%	2,8	2,8	20.02	392	0.72
		30%	2,8	2,8	24.54	143	0.64
26	Copter	10%	2,8	2,8	21.34	374	0.42
		20%	2,8	2,8	23.15	102	0.78
		30%	2,8	2,8	25.32	71	0.73
27	Brodatz	10%	2,8	2,8	21.49	406	0.13
		20%	2,8	2,8	20.51	87	0.74
		30%	2,8	2,8	21.86	387	0.25
28	Scene2	10%	2,8	2,8	19.10	246	0.55
		20%	2,8	2,8	19.93	361	0.47
		30%	2,8	2,8	18.36	157	0.79
29	Scene3	10%	2,8	2,8	17.13	686	0.68
		20%	2,8	2,8	24.51	84	0.25
		30%	2,8	2,8	22.87	133	0.62
30	Scene4	10%	2,8	2,8	20.98	411	0.77
		20%	2,8	2,8	18.11	972	0.37
		30%	2,8	2,8	16.71	120	0.46

Table A.15: Results of stochastic resonance based mean shift filtering(contd..)

S.No.	Image	Gaussian Noise	σ_s	σ_r	PSNR	Region Count	Pratts Fig-of-merit
31	Scene5	10%	2,8	2,8	26.35	982	0.73
		20%	2,8	2,8	26.06	101	0.73
		30%	2,8	2,8	22.62	303	0.74
32	Scene6	10%	2,8	2,8	20.62	237	0.75
		20%	2,8	2,8	15.61	370	0.46
		30%	2,8	2,8	18.25	1477	0.57
33	Scene7	10%	2,8	2,8	22.97	753	0.69
		20%	2,8	2,8	20.56	251	0.61
		30%	2,8	2,8	18.58	1101	0.80
34	Space1	10%	2,8	2,8	19.11	72	0.73
		20%	2,8	2,8	23.37	117	0.74
		30%	2,8	2,8	20.08	136	0.30
35	Space2	10%	2,8	2,8	20.81	935	0.67
		20%	2,8	2,8	17.52	442	0.32
		30%	2,8	2,8	20.39	2282	0.42
36	Tree	10%	2,8	2,8	21.39	239	0.47
		20%	2,8	2,8	23.02	569	0.30
		30%	2,8	2,8	24.18	853	0.53
37	Vegetables	10%	2,8	2,8	22.87	1300	0.66
		20%	2,8	2,8	22.91	251	0.82
		30%	2,8	2,8	20.79	303	0.76
38	Bird	10%	2,8	2,8	28.95	168	0.79
		20%	2,8	2,8	25.37	116	0.73
		30%	2,8	2,8	17.71	34	0.69
39	Barco	10%	2,8	2,8	12.40	333	0.27
		20%	2,8	2,8	21.05	99	0.68
		30%	2,8	2,8	18.61	95	0.68
40	Lizard	10%	2,8	2,8	21.06	286	0.65
		20%	2,8	2,8	22.47	181	0.65
		30%	2,8	2,8	25.62	156	0.68